Analysis of GLUT4 Distribution in Whole Skeletal Muscle Fibers: Identification of Distinct Storage Compartments That Are Recruited by Insulin and Muscle Contractions

Thorkil Ploug,*‡∥ Bo van Deurs,§ Hua Ai,*‡ Samuel W. Cushman,∥ and Evelyn Ralston¶

*Copenhagen Muscle Research Centre, Rigshospitalet; ‡Department of Medical Physiology and §Structural Cell Biology Unit, Department of Medical Anatomy, The Panum Institute, University of Copenhagen, DK-2200 Copenhagen N, Denmark; ∥Experimental Diabetes, Metabolism, and Nutrition Section, Diabetes Branch, National Institute of Diabetes and Digestive and Kidney Diseases; and ¶Laboratory of Neurobiology, National Institute of Neurological Disorders and Stroke, National Institutes of Health, Bethesda, Maryland 20892-4062

Abstract. The effects of insulin stimulation and muscle contractions on the subcellular distribution of GLUT4 in skeletal muscle have been studied on a preparation of single whole fibers from the rat soleus. The fibers were labeled for GLUT4 by a preembedding technique and observed as whole mounts by immunofluorescence microscopy, or after sectioning, by immunogold electron microscopy. The advantage of this preparation for cells of the size of muscle fibers is that it provides global views of the staining from one end of a fiber to the other and from one side to the other through the core of the fiber. In addition, the labeling efficiency is much higher than can be obtained with ultracryosections. In nonstimulated fibers, GLUT4 is excluded from the plasma membrane and T tubules. It is distributed throughout the muscle fibers with ∼23% associated with large structures including multivesicular endosomes located in the TGN region, and 77% with small tubulovesicular structures. The two stimuli cause translocation of GLUT4 to both plasma membrane and T tubules. Quantitation of the immunogold electron microscopy shows that the effects of insulin and contraction are additive and that each stimulus recruits GLUT4 from both large and small depots. Immunofluorescence double labeling for GLUT4 and transferrin receptor (TfR) shows that the small depots can be further subdivided into TfR-positive and TfR-negative elements. Interestingly, we observe that colocalization of TfR and GLUT4 is increased by insulin and decreased by contractions. These results, supported by subcellular fractionation experiments, suggest that TfR-positive depots are only recruited by contractions. We do not find evidence for stimulation-induced unmasking of resident surface membrane GLUT4 transporters or for dilation of the T tubule system (Wang, W., P.A. Hansen, B.A. Marshall, J.O. Holloszy, and M. Mueckler. 1996. *J. Cell Biol.* 135:415–430).

Key words: membrane trafficking • glucose transport • endosomes • exercise • diabetes

SKELETAL muscle plays a major role in maintaining homeostasis of blood glucose. It uses glucose as a source of energy during contractile activity, and represents the major disposal site for insulin-stimulated glucose metabolism during the postprandial phase (Katz et al., 1983; DeFronzo et al., 1992). The rate-limiting transport of glucose across cell surface membranes is mediated by tissue-specific members of the facilitative glucose transporter family, of which GLUT4 is the major isoform in skeletal muscle (Bell et al., 1993). Unlike other isoforms which constitutively reside in the cell surface membrane, GLUT4 is stored intracellularly (Pascoe et al., 1996). Studies carried out initially in adipose cells (Cushman and Wardzala, 1980; Suzuki and Kono, 1980) and later in skeletal muscle (Wardzala and Jeanrenaud, 1981; Douen et al., 1990) suggested that insulin-stimulated glucose transport results from a regulated exocytosis of GLUT4 from intracellular storage sites to the cell surface (Birnbaum, 1992). This model is now well supported, qualitatively and quantitatively, by biochemical as well as morphological studies in both white and brown adipose cells (Slot et al., 1991a; Holman and Cushman, 1994), and cardiac myocytes (Slot et al., 1991b, 1997). There is evidence for GLUT4 translocation in skeletal muscle as well, but the morphological

Address all correspondence to T. Ploug, Department of Medical Physiology, The Panum Institute, University of Copenhagen, Blegdamsvej 3C, DK-2200 Copenhagen N, Denmark. Tel.: (45) 35-32-74-35. Fax: (45) 35-32-74-20. E-mail: t.ploug@mfi.ku.dk

studies have been less extensive and qualitative only (Bornemann et al., 1992; Rodnick et al., 1992; Takata et al., 1992).

Specific properties make skeletal muscle more complex than the other insulin-responsive tissues. In addition to insulin, muscle contractions also increase glucose transport in skeletal muscle and the effects of the two stimuli are additive (Nesher et al., 1985; Ploug et al., 1987; Constable et al., 1988). Consistent with the additive nature of the two stimuli, insulin and contractions have been found to recruit GLUT4 from different intracellular pools (Douen et al., 1990; Coderre et al., 1995). Since the main intracellular storage sites for GLUT4 include the *trans*-Golgi network (TGN) region and tubulovesicular structures, often just beneath the cell surface (Slot et al., 1991a,b), it seems likely that these two types of storage sites could represent the two pools. But, surprisingly, even after immunoadsorption, no difference in the protein composition of the two pools could be detected, although the insulin-sensitive GLUT4 vesicles had a larger sedimentation coefficient than the exercise-sensitive vesicles on a sucrose velocity gradient (Coderre et al., 1995). More recently, it has been observed that GLUT4 vesicles were recruited by insulin from a muscle subcellular fraction devoid of endosomal markers such as the transferrin receptor (TfR)[1] (Aledo et al., 1997; Sevilla et al., 1997), which suggests a possible basis for identification of the pools.

The subcellular architecture of skeletal muscle is very different from that of mononucleated cells. Muscle fibers contain up to several thousand nuclei derived from the fusion of myoblasts in fetal and postnatal life. During myogenesis, the Golgi complex disperses into elements that migrate to a perinuclear position and to sites scattered throughout the cytoplasm (Tassin et al., 1985; Ralston, 1993; Rahkila et al., 1997). GLUT4 has been found associated with Golgi complexes/TGN in skeletal muscle (Bornemann et al., 1992; Rodnick et al., 1992; Takata et al., 1992; Ralston and Ploug, 1996a; Rahkila et al., 1998), but the extent of this association is not clear. Furthermore, the muscle surface membrane consists of two distinct domains, the plasma membrane proper and the T tubules. The best known function of the T tubules is to rapidly spread changes in membrane potential throughout the muscle fibers. By analogy, T tubules might also serve as irrigation channels to provide the extracellular fluid direct access to the core of the thick muscle fibers. In agreement with this view, GLUT4 transporters have been found associated with T tubules (Dohm et al., 1993; Munoz et al., 1995; Wang et al., 1996) and subcellular fractionation experiments suggest that both insulin and contractions translocate GLUT4 to the T tubule membrane (Marette et al., 1992; Munoz et al., 1995; Roy and Marette, 1996). Intriguingly, however, GLUT4 translocation to the T tubules has never been demonstrated morphologically in skeletal muscle, in contrast to the situation in cardiac myocytes (Slot et al., 1991b).

Despite the lack of a comprehensive and quantitative morphological analysis, it is generally believed that trans-

location of GLUT4 in skeletal muscle is similar to that described in adipocytes and cardiac myocytes. However, it has recently been suggested that insulin primarily stimulates glucose transport in skeletal muscle, not through translocation, but through unmasking of resident GLUT4 transporters in the T tubule membrane concomitant with dilation of the T tubule lumen (Wang et al., 1996). This provocative hypothesis is based on immunocytochemical studies of muscle sections from GLUT4-overexpressing transgenic mice. It challenges the concept that upon stimulation, GLUT4 translocates from intracellular stores to the surface membrane in all insulin-responsive cells, including skeletal muscle. The notion that the COOH-terminal epitope of GLUT4 may be masked in unstimulated cells was introduced in an earlier study of rat adipose cells (Smith et al., 1991) and was never settled.

In an attempt to solve the riddle of glucose transport in skeletal muscle, we have carried out an extensive study of the localization of endogenous GLUT4 in rat skeletal muscle. We have taken advantage of a preparation of whole mount muscle fibers which allows the study of large continuous areas of fibers by both light (LM) and electron microscopy (EM). In nonstimulated fibers, GLUT4 is distributed throughout the muscle fibers with ~23% located in large structures including large endosomes in the TGN region and the remaining with small tubulovesicular structures. Stimulation with insulin and muscle contraction results in an additive translocation of GLUT4 to both plasma membrane and T tubules. Both large and small depots are affected by each stimulus. The large depots are primarily attenuated in size, whereas the small depots are reduced in number. We find that the small depots can be further subdivided into TfR-positive and -negative elements. Interestingly, TfR-positive elements are selectively recruited by contractions and TfR-negative elements by insulin. We have also estimated the relative number of GLUT4 epitopes accessible to antibodies against both NH$_2$- and COOH-terminal peptides by measuring the amount of secondary ^{125}I-labeled antibody bound to single muscle fibers. We do not find any evidence of stimulation-induced unmasking of GLUT4 epitopes or of stimulation-induced dilation of the T tubule system.

Materials and Methods

Animal Procedures

Male Wistar rats (300–350 g), obtained either from the Charles River Breeding Laboratories (Boston, MA) or from the breeding facilities at the Panum Institute, were anesthetized by intraperitoneal injection of sodium pentobarbital (5 mg per 100 g of body weight) and assigned to one of four groups. The control (Bas) and the contraction (Ex) groups received 0.7 ml saline as a bolus injection in a tail vein 20 min before fixation. The insulin (I) and the insulin plus contraction (ExI) groups received a tail vein bolus injection of 0.5 ml of 50% glucose followed by 20 U (0.2 ml) insulin (Actrapid human; Novo Nordisk, Bagsvaerd, Denmark). 9 min later, hindleg muscles of rats in the Ex and ExI groups were electrically stimulated by tetanic contractions for two periods of 5 min each separated by 1 min of rest. Electrodes were inserted in the feet and through the skin in the posterior hip region close to the sciatic nerve. Stimulation was given as 200 ms trains of 100 Hz, each impulse lasting 0.2 ms, one train delivered per second at a supramaximal voltage (Ploug et al., 1987). Immediately after the 20-min stimulation period, a canula was placed in the descending aorta and the inferior vena cava was cut open. The hindquarters were perfused with 150 ml of cold Krebs-Henseleit bicarbonate buffer containing

---

1. *Abbreviations used in this paper*: LM, light microscopy; SR, sarcoplasmic reticulum; TfR, transferrin receptor.

procaine hydrochloride (1 g/liter) for 1.5 min (Bornemann et al., 1992) followed by 900 ml of 2% freshly depolymerized paraformaldehyde, in some experiments supplemented with 0.15% picric acid (Stefanini et al., 1967), in 0.1 M Sorensens phosphate buffer at 2°–6°C for 9 min. The soleus muscles were excised, left for an additional 5 h in the perfusion fixative at 4°C, and then transferred to pH 7.3 PBS.

Antibodies

P-1 is a polyclonal rabbit antibody raised against a synthetic peptide corresponding to the COOH-terminal 13 amino acids of GLUT4 (Ploug et al., 1990). Affinity-purified P-1 was used at a concentration corresponding to a ~1:1,000 dilution of crude serum. Its specificity in immunocytochemical staining was confirmed by peptide competition at both LM and EM levels. Additional staining controls included omission of primary antibody. MCB2, a generous gift from M. Charron (Albert Einstein College of Medicine, Bronx, NY), is a polyclonal rabbit antibody raised against a synthetic peptide corresponding to the 13 NH_2-terminal amino acids of GLUT4 (Kahn et al., 1991; Smith et al., 1991). MCB2 was used as crude serum diluted 1:500. A hybridoma supernatant of the anti-TGN38 mouse monoclonal antibody 2F7.1 (Horn and Banting, 1994) was kindly donated by K.E. Howell (University of Colorado Health Sciences Center, Denver, CO) and used at a dilution of 1:25. A hybridoma supernatant of the mouse monoclonal antibody H68.4 recognizing human and rat TfR was kindly donated by I. Trowbridge (Salk Institute, San Diego, CA) (White et al., 1992) and used at a dilution of 1:50. A rabbit polyclonal antibody against rat caveolin-3 (Transduction Laboratories, Inc., Lexington, KY) was used at a dilution of 1:500.

Teased Fibers Preparation and Staining for Fluorescence and EM

Bundles of 1–3 individual fibers were teased from fixed muscles with fine forceps and transferred to 50 mM glycine in PBS. Nonspecific binding was blocked with 50 mM glycine, 0.25% bovine serum albumin, 0.03% saponin, and 0.05% sodium azide in PBS for 30 min. Fibers were then incubated overnight with the primary antibody diluted in blocking buffer supplemented with 200 µg/ml goat IgG. After three washes of 30 min each they were incubated for 2 h with FITC-conjugated goat anti–rabbit F(ab)₂ fragments (Sigma Chemical Co., St. Louis, MO) diluted 1:250 in blocking buffer. For double labeling, biotin-coupled goat anti–mouse IgG was added (1:500; Pierce Chemical Co., Rockford, IL) after three washes by Texas red–conjugated streptavidin (2 µg/ml, Pierce Chemical Co.) and Hoechst 33342 (0.5 µg/ml) in blocking buffer. Fibers were mounted in Vectashield on a glass slide, examined, and then photographed with a Zeiss Axioskop (Carl Zeiss, Inc., Thornwood, NY) or a Leica DMRD (Leica USA, Deerfield, IL).

For electron microscopy, the secondary antibody incubation was for 2 h with goat anti–rabbit Fab fragments conjugated to 1.4–nm gold clusters (Nanoprobes Inc., Stony Brook, NY) diluted 1:300 in blocking buffer. Fibers were washed in blocking buffer followed by PBS, and fixed for 1 h at room temperature in 2.2% glutaraldehyde in 0.1 M phosphate buffer, pH 7.3. After several washes in water, silver enhancement (HQ Silver; Nanoprobes Inc.) was carried out for 6 min, followed by washes in water and overnight storage in 0.1 M phosphate buffer at 4°C. Fibers were treated with 0.5% osmium tetroxide in 0.1 M phosphate buffer for 20 min, en block mordanted for 15–20 min in 2% uranyl acetate in 50% acetone, dehydrated in a graded series of acetone, infiltrated with epoxy resin Polybed 812 (Polysciences Inc., Warrington, PA), horizontally embedded in flat molds, and then cured for 2 or 3 d at 55°C. Silver–gold interference-colored sections were examined in a JEOL 1200 microscope (JEOL USA, Peabody, MA) at 60 kV. Sections were usually poststained for 5 min with aqueous lead citrate.

Cryosection Procedures

The Tokuyasu technique was used (Tokuyasu, 1980, 1989). Fixed muscles were cut into small pieces and then infiltrated with a mixture of 1.8 M sucrose and 20% (wt/vol) polyvinylpyrrolidone in 0.1 M phosphate buffer, pH 7.3, overnight at 4°C. Muscle pieces were mounted on specimen stubs and frozen in liquid nitrogen.

For immunofluorescence, sections ~400-nm thick were cut on an Ultracut FCS ultracryomicrotome (Leica Microsystems, Herlev, Denmark) and transferred with thawing on a drop of 2.3 M sucrose in PBS to Teflon-coated glass slides with circular wells. The sections were first quenched with 50 mM glycine in PBS for 10 min followed by incubation with blocking buffer for 30 min. Sections were incubated for 90 min with primary antibodies diluted in the same, washed three times for 10 min each in PBS followed by a 1-h incubation with appropriate biotinylated secondary antibody, and then washed and incubated for 15 min with FITC-streptavidin and Hoechst 33342, washed three times for 10 min each in PBS, and then mounted in Vectashield.

For electron microscopy, sections ~80-nm thick were cut on an Ultracut FCS ultracryomicrotome and transferred with thawing on a drop of 2.3 M sucrose to formvar-coated nickel grids. Grids were placed on drops of cryo buffer (5% fetal calf serum in PBS plus 20 mM glycine) for 15 min, transferred to cryo buffer containing P-1 diluted 1:250 for 45 min, washed six times for 3 min each in cryo buffer, incubated on drops of goat anti–rabbit IgG or protein A adsorbed to 5-nm gold particles or on drops of goat adsorbed to 5-nm colloidal gold particles or goat anti–rabbit Fab fragments conjugated to 1.4-nm gold clusters (Nanoprobes Inc.) diluted 1:500 in CB for 30 min, washed four times for 3 min each in CB and four times for 3 min in PBS and placed on drops of 1% glutaraldehyde in PBS for 10 min. Grids were rinsed six times on drops of distilled water, placed on drops of silver enhancement reagent for 3.5–4 min, rinsed six times on drops of distilled water, treated with 2% neutral pH uranyl acetate oxalate for 5 min, rinsed three times in distilled water, incubated on drops of ice-cold 0.25% uranyl acetate in 2% methyl cellulose for 10 min, blotted, and then air dried. Sections were examined in a JEOL 100 CX microscope at 80 kV.

For quantitation of the electron microscopy experiments, sections were screened at low magnification and those that contained at least three different fibers were analyzed further. Random areas of each fiber were selected at low magnification, then observed at 12,000 primary magnification and photographed, unless the plasma membrane appeared damaged. Silver-enhanced gold grains were counted from the surface to a depth of 4 µm inside the fibers with the use of a magnifying glass in order to facilitate the counting of single grains in areas with a very high labeling density. The depth cutoff was well within the range of maximum penetration of the labeling reagents.

Confocal Image Acquisition and Analysis

Confocal images were collected in the NINDS Light Imaging Facility on a Micro Systems LSM 520 equipped with a Zeiss LSM 410 microscope equipped with an Axiovert TV microscope (Carl Zeiss, Inc.). Settings were adjusted so that images of control fibers stained without primary antibody appeared essentially black. Images recorded for pattern observation or determination of colocalization were recorded with settings that maximized the brightness of the smaller staining elements, often resulting in saturation of the brightest elements (see Figs. 2, 3, 10, and 11). In contrast, for quantitation or comparison of the different stimulations, all images were recorded with identical settings that avoided saturation of the brightest pixels (see Figs. 6 and 9).

To facilitate the recording of large numbers of random images, fibers were mounted in two rows of 10–12 fibers each, roughly parallel to one another. The fibers were localized at low magnification by the UV fluorescence of the Hoechst-stained nuclei and an area was arbitrarily decided upon. The stage was then only moved in the direction perpendicular to the long axis of the fibers, and an image was randomly collected from each fiber, with lateral movement of the stage only as needed to find en face nuclei.

For recordings from double-labeled fibers, registration of the two channels was verified by recording images from red and green fluorescent 1-µm beads. Images were recorded independently and combined electronically. To produce the cartoon shown in Fig. 10, the single recordings were imported into the public domain program NIH Image (written by W. Rasband at the National Institutes of Health and available from the Internet by anonymous FTP from zippy@nimh.nih.gov). A black-and-white binary picture was obtained by thresholding. To include the weakly stained elements without artificially increasing the size of the brighter ones, three levels of thresholding were determined manually. From the three views a single composite image was created that included each staining element in its sharpest form. The binary image was imported into Photoshop 3.0.5 (Adobe Systems, Inc., Mountain View, CA), contoured, combined with the contoured image from the other recording, and then printed on a Fuji Pictrography 3000 printer (Tokyo, Japan). All the quantitation and image analysis was performed on a Power Macintosh computer. To quantitate overlap of GLUT4 and TfR staining, each separate image, covering one nucleus recorded at high magnification (100×; N.A.1.4 lens, zoom 2.4) was imported into NIH Image, inverted, thresholded automatically, and

then made into a binary black-and-white image. The image representing the overlap of the two binary images was calculated. For each nucleus, the number of black pixels within the perinuclear fence was calculated and expressed as the percent of the number of black pixels in the corresponding area of the GLUT4 image. It is important to keep in mind that this way of calculating is purely geometrical and that the initial thresholding erases differences in relative staining intensities.

Preparation of Subcellular Membrane Fractions and Western Blotting

Muscle microsomal membranes were prepared from mixed rat hindlimb muscles as described previously (Ploug et al., 1992) with a few modifications. During the incubation with DNase the following protease inhibitors were added (final concentration): 2.1 mM PMSF, 1.5 mM AEBSF, 12.5 μg/ml pepstatin A, 20 μg/ml leupeptin, and 20 μg/ml antipain. Furthermore, the overnight density gradient separation was carried out using a SW 28.1 rotor (Beckman Instrs., Palo Alto, CA) operating at 28,000 rpm. Membranes were resuspended in 29% Nycodenz, overlayed by 3 ml of 23%, 3 ml of 21%, 3 ml of 17%, 3 ml of 12% Nycodenz and 1.5 ml of buffer. Separation was done for 12–14 h at 28,000 rpm. Fraction 1 (F1)–fraction 4 (F4) were collected at the buffer/12%, 12%/17%, 17%/21%, and 21%/23% interfaces, respectively.

5–15 μg of protein were separated by SDS-PAGE and electrophoretically transferred to PVDF membranes, incubated with primary antibody followed by ^{125}I-labeled secondary antibody, and then quantitated with a PhosphorImager (Ploug et al., 1997).

Results

Immunofluorescence Labeling of GLUT4 in Whole Mounts of Nonstimulated Fibers Reveals Localization in Large and Small Clusters, Both near the Surface and in the Core of the Fibers

The staining of transverse cryostat sections of unfixed rat soleus muscle (Ralston and Ploug, 1996b) shows that the concentration of GLUT4 is highest at the periphery of the fibers but that discrete staining is also seen throughout their core. The distribution and intensity of staining for GLUT4 is similar in all fibers but the low resolution of the cryostat technique does not allow identification of the staining elements or differentiation between labeling of the plasma membrane itself and of subsarcolemmal structures.
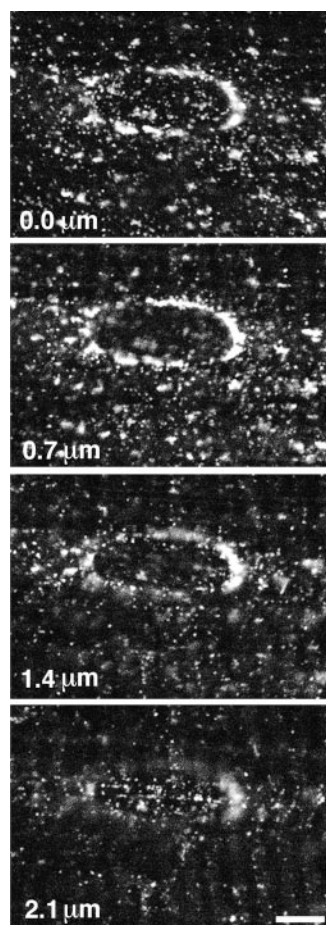
A much better image is obtained when single basal fibers[2] stained for GLUT4 are observed as whole mounts

---

2. In the text, we refer to fibers prepared from basal, nonstimulated soleus muscle as basal fibers, and to fibers from insulin-stimulated muscle as insulin-stimulated fibers, etc.
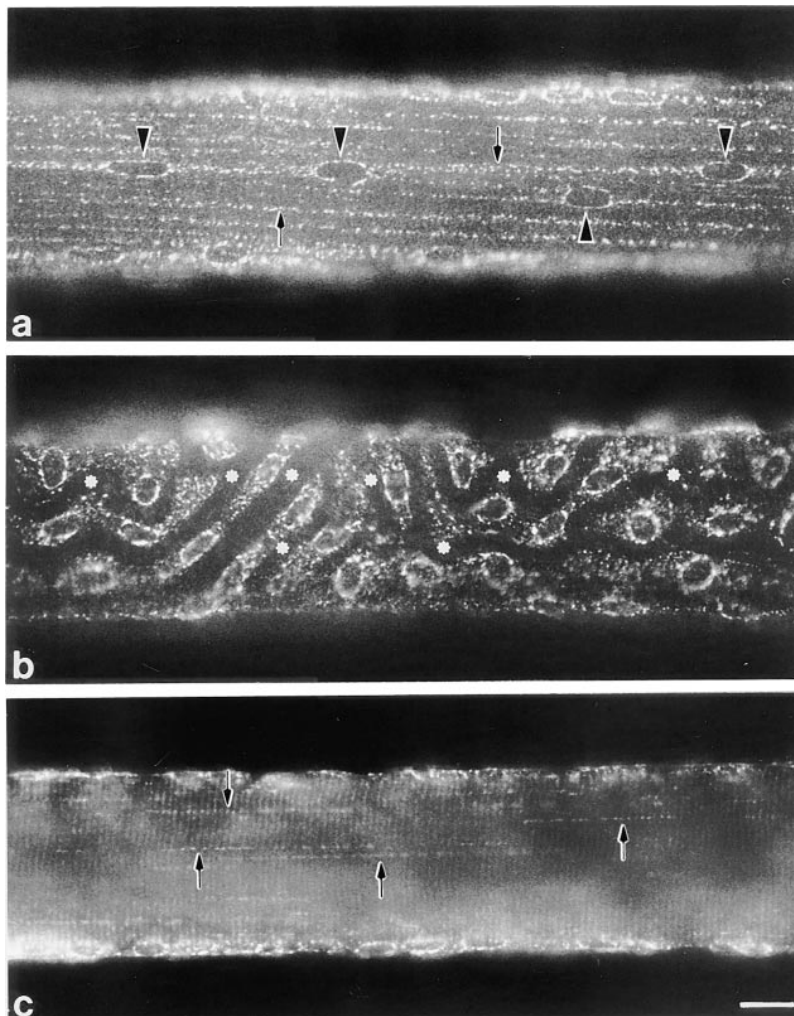
Figure 1. Immunofluorescence localization of GLUT4 in single fibers from basal soleus muscle. Single fibers were stained with anti-GLUT4 antiserum followed by biotin-conjugated anti-rabbit IgG and FITC-labeled streptavidin. (*a*) At the surface of the fibers, in some areas, myonuclei (*arrowheads*) are aligned with the axis of the fiber and joined by regular rows of GLUT4 aggregates (*arrows*). (*b*) In other areas, nuclei are not aligned with the axis of the fiber and the staining pattern appears less orderly. Dark channels (*asterisks*) correspond to capillaries. (*c*) In the core of the fibers, the staining consists of dotted lines (*arrows*) and weak cross-striations. Bar, 10 μm.

by immunofluorescence at low or intermediate magnification. Fig. 1 gives examples of the striking pattern apparent when focusing on the thin layer of cytoplasm just below the surface of the fibers. The oval nuclei are surrounded with GLUT4 staining. In areas such as that shown in Fig. 1 *a*, the oval nuclei are aligned parallel to the fiber axis and appear like beads on strings made up of GLUT4 aggregates (Fig. 1 *a*, *arrows*). These strings can be followed over remarkable distances, linking nuclei hundreds of microns apart. In contrast, there are areas of fibers (Fig. 1 *b*), where the arrangement of nuclei and GLUT4 aggregates appears disorganized, with dark channels (*asterisks*) along which the nuclei are positioned. Although Fig. 1, *a* and *b* were taken from different fibers, the two types of patterns coexist and blend into one another in each single fiber (data not shown). The dark channels are in fact blood vessels of the highly vascularized red soleus muscle (Ranvier, 1874). They follow a tortuous course, along and across the muscle fibers as can be seen by phase-contrast of whole mounts (data not shown). The two GLUT4 patterns correspond to fiber segments without blood vessels (Fig. 1 *a*) and with blood vessels (Fig. 1 *b*), respectively. The same pattern is observed in muscles fixed by immersion (data not shown), which rules out that the nuclei are dislodged as a consequence of dilation of the blood vessels during the perfusion fixation. When the plane of focus is deeper in the core of the fiber (Fig. 1 *c*), we observe rows of dots parallel to the fiber axis (*arrows*) together with weaker cross-striations, the periodicity of which corresponds to the periodicity of the sarcomeres. There is no continuous staining of the plasma membrane.

At higher resolution (Fig. 2), GLUT4 staining can be separated, somewhat arbitrarily, into two categories of elements based on size: (*a*) large, rather irregular intense dots which form the discontinuous belt around the nuclei and the string-like staining already noticed, and (*b*) a finer punctate and tubular staining found both near the surface and in the core of the fibers.

Using confocal z series consisting of 1-μm-thick optical sections through the upper half of muscle fibers, we have calculated that $68 \pm 1\%$ (mean $\pm$ SE, $n = 3$) of the total GLUT4 staining is associated with the superficial 3-μm cy-
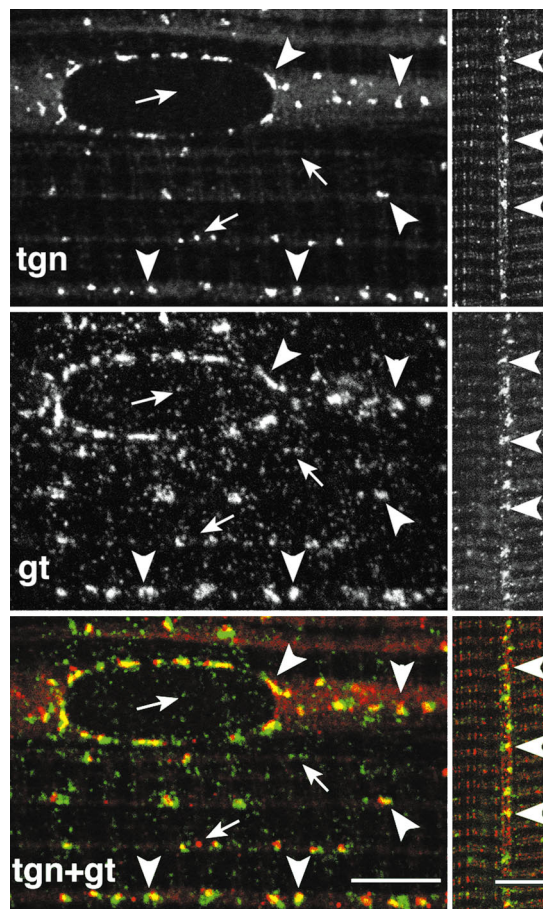

Figure 2. High magnification view of GLUT4 immunofluorescence in basal muscle fibers. Single fibers were stained as described in Fig. 1. A series of confocal images, centered on a nucleus, were recorded from the surface of the fiber (0.0 μm) and at depths of 0.7, 1.4, and 2.1 μm. GLUT4 is present in numerous small tubulovesicular structures and in larger perinuclear elements that form a belt around the nucleus. Bar, 5 μm.

Figure 3. The large, but not the small depots of GLUT4, are close to the TGN at the surface and in the core of basal fibers. Single basal fibers were stained simultaneously with an antibody to TGN38 (*tgn*) followed by a Texas red–conjugated secondary antibody and to GLUT4 (*gt*) followed by a fluorescein-conjugated secondary antibody. Single confocal images were recorded, separately for each fluorophore, from the surface (*left panels*) or the core (*right panels*) of the fibers. The inside views were rotated by 90° compared with the surface views, explaining why the striations are horizontal. When the *green* and *red* images are superimposed and viewed in color, their overlap, shown in *yellow*, is only partial. The smaller depots of GLUT4 have no corresponding TGN staining and an occasional TGN has no visible GLUT4 (*small arrows*, orphan structures). However, in both areas, each of the large depots of GLUT4 has a TGN counterpart (*arrowheads*, some of the corresponding elements). Bars, 5 μm.
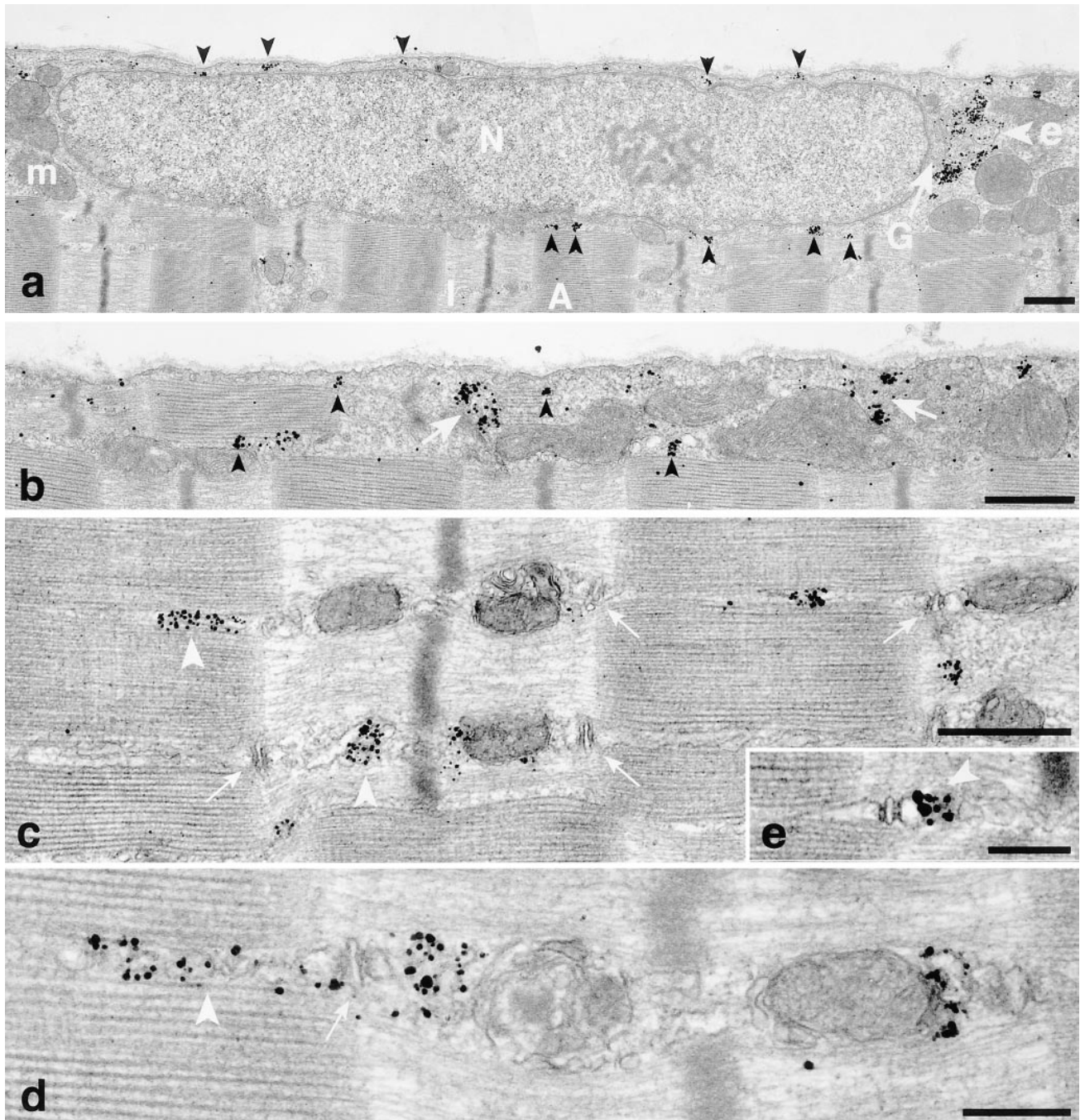
toplasmic layer and the remaining 32% with the deeper region of the fiber, confirming the general impression from cryostat sections (Ralston and Ploug, 1996b). Dividing the GLUT4 staining into either large or small elements, as defined in the preceding paragraph, we find that the large ones account for 23 ± 0.3% (mean ± SE, $n = 3$) of the total GLUT4 staining, compared with 77% for the smaller, more symmetrical GLUT4-containing structures.

Large Clusters of GLUT4 Are Close to the TGN

Previous studies at the EM level have observed that part of GLUT4 is associated with the Golgi complex or TGN (Bornemann et al., 1992; Rodnick et al., 1992a; Takata et al.,

1992). Furthermore, the perinuclear pattern of GLUT4 staining at the LM level (refer to Fig. 1) resembles that observed with markers of the Golgi complex in muscle (Ralston, 1993; Rahkila et al., 1996). To assess if all large depots of GLUT4, including those in the core of the fibers, are associated with stacks of Golgi cisternae, we stained basal fibers simultaneously with anti-GLUT4 and with anti-TGN38 (Luzio et al., 1990). The TGN38 staining (Fig. 3) shows a pattern similar to that of the large GLUT4 clusters, but none of the finer punctate staining. When the two images are superimposed, there is a partial overlap of the two markers in the large GLUT4 depots. The partial overlap is observed both in the subsarcolemmal cytoplasm (Fig. 3, *left panels*) and in the myofibrillar region (Fig. 3,
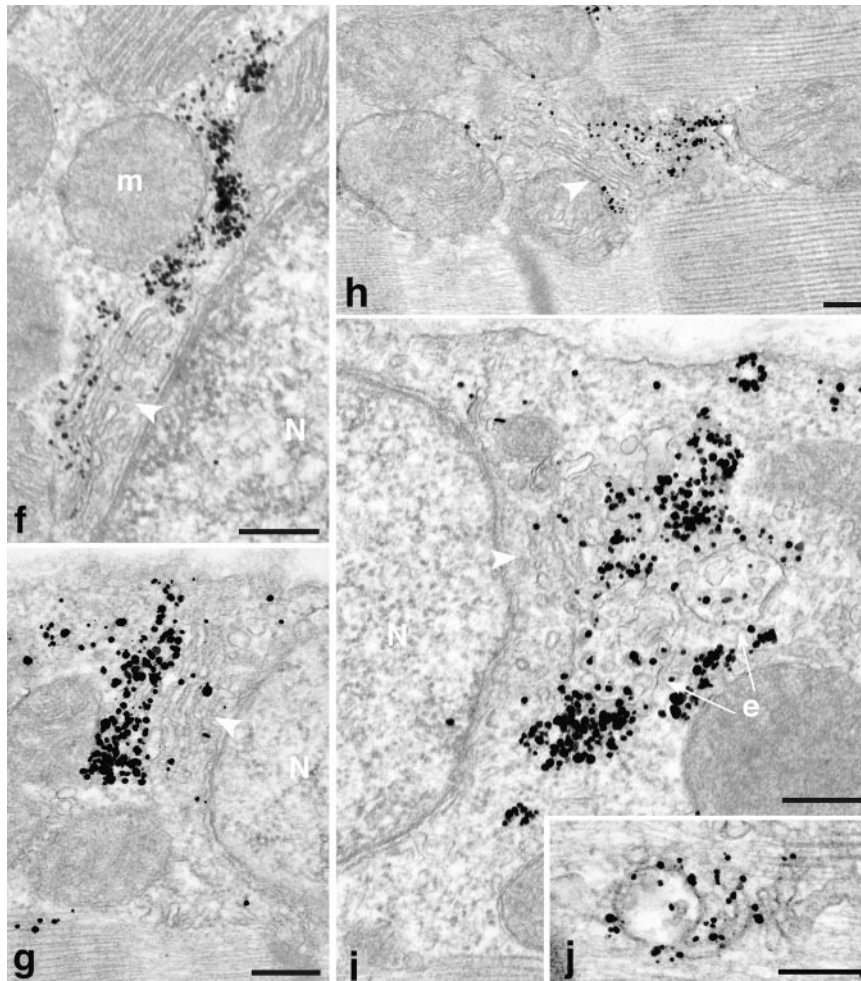
Figure 4. Localization of GLUT4 in basal fibers observed by preembedding immunogold electron microscopy. Single fibers were stained and embedded in epoxy resin as described in Materials and Methods. (*a* and *b*) Low magnification views of two areas close to the plasma membrane, one with a nucleus (*a*), the other with myofibrils extending very close to the plasma membrane (*b*). Both show small (*arrowheads*) and large (*arrow*) clusters of GLUT4. In *a* they surround a nucleus (*N*). The large clusters are next to a Golgi complex (*G*) and to multivesicular bodies (*e*; see enlarged area in *i*). Other recognizable elements are mitochondria (*m*) and myofibrils that fill the core of the fiber, with the characteristic A and I band alternation. Note the almost complete absence of single grains on the plasma membrane. (*c*–*e*) Distribution of GLUT4 in the core of the fibers. In basal conditions, most GLUT4 staining is in clusters of grains (*arrowheads*) in the I band, near the A–I band intersection, or more rarely in the A band. T tubules at the triad junctions (*small arrows*) are unlabeled but there is labeling of terminal cisternae of the SR (*d* and *e*) and of what appears to be the fenestrated SR in the A band (*arrowheads*). (*f*–*j*) Details of GLUT4 localization showing association with Golgi complex and endosomes. (*f*–*g*) Next to nuclei (*N*) that are close to the fiber surface, stacks of Golgi cisternae (*arrowheads*) can be recognized. GLUT4 is concentrated in the cisternae farthest away from the nucleus and in tubulovesicular structures just beyond or lateral to the cisternae. In *h*, GLUT4 is associated with a Golgi complex which is in the myofibrillar core and is not associated with a nucleus. In *i*, the gold grains are next to Golgi cisternae and to mutivesicular bodies, presumably endosomes (*e*), whereas *j* shows an abundantly labeled endosome in the myofibrillar core. Bars: (*a*–*c*) 0.5 μm; (*d*–*j*) 0.2 μm.

right panels). The limited character of the overlap and the slightly different shape of the staining suggest that GLUT4 and TGN38 may occupy compartments that are very close to one another but separate. The important point is that for nearly each of the large GLUT4 depots, there seems to be a corresponding TGN38 staining. A similar correspondence was observed between GLUT4 and GM130, a protein of the *cis*-Golgi complex (Nakamura et al., 1995) (data not shown).

At the EM level, the GLUT4 labeling observed at low magnification in basal fibers (Fig. 4, *a* and *b*) can be classified into large (*arrows*) and small (*arrowheads*) structures, just like in immunofluorescence. Numerous small GLUT4 clusters are also located in the myofibrillar region, in the I band, at the I–A band junction, and in the A band (Fig. 4, *a*–*e*). GLUT4 staining is also occasionally seen on what appears to be longitudinally oriented fenestrated sarcoplasmic reticulum (SR) in the A-band (Fig. 4, *c* and *d*) and on terminal cisternae of the SR (Fig. 4, *d* and *e*). However, double labeling experiments with SR-specific markers will be required for unambiguous verification. Only very few gold grains are seen on the plasma membrane (Fig. 4, *a*

and *b*) and GLUT4 is excluded from the T tubules at the triadic junctions (Fig. 4, *c*–*e*). There is a high concentration of GLUT4 in the TGN area (Fig. 4, *f*–*h*), presumably corresponding to the perinuclear staining observed in LM. The label is concentrated in the cisternae distal from the nucleus and in vesicles beyond, which together define the TGN (Griffiths and Simons, 1986; Mellman and Simons, 1992). Stacks of Golgi cisternae with GLUT4 labeling are often seen far from any nucleus, both in the cytoplasm and in the myofibrillar region (Fig. 4 *h*). Multivesicular bodies, most likely endosomes (see Fig. 12), are also seen both in the cytoplasm (Fig. 4 *i*) and in the myofibrillar region (Fig. 4 *j*). They are surrounded by dense GLUT4 labeling on tubulovesicular structures. The internal vesicles of the multivesicular bodies show some labeling as well (Fig. 4, *i* and *j*).

Thus, in agreement with previous studies (Bornemann et al., 1992; Rodnick et al., 1992; Takata et al., 1992), GLUT4 appears to be essentially excluded from both domains of the surface membrane of basal muscle fibers but is found in the TGN region, associated with endosomes, and in small tubulovesicular structures in the subsarcolemmal cytoplasm as well as in the myofibrillar core.
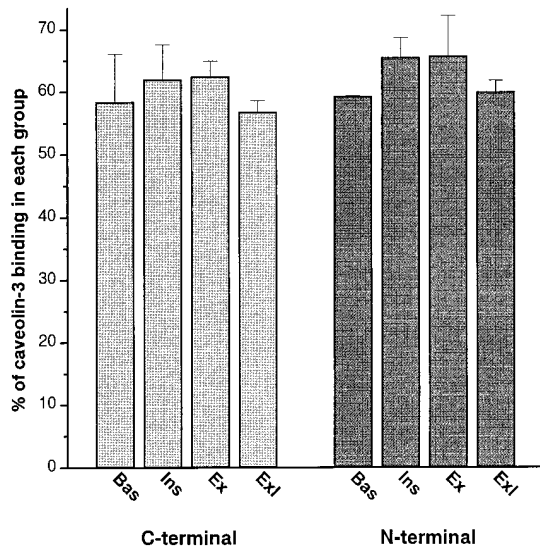
Figure 5. Insulin and muscle contractions do not affect accessibility of GLUT4 NH_2- or COOH-terminal epitopes. Teased single fibers, each ~9-mm long, were prepared from basal (*Bas*), insulin- (*Ins*), contraction- (*Ex*) and insulin- and contraction-stimulated muscles (*ExI*). They were permeabilized and stained with antibodies to the COOH- or NH_2-terminal part of GLUT4 or to caveolin-3. Primary antibody binding was quantitated by measuring the amount of ^{125}I-labeled secondary antibody binding. Amount of bound GLUT4 antibodies is expressed as percent of caveolin-3 binding to fibers from the same muscle in order to correct for possible variations in sarcomere length during fixation. Results are presented as mean $\pm$ SEM of two or three separate experiments with 10–15 fibers per experiment. Analysis of variance (ANOVA) did not detect any significant difference between stimulation states within each antibody group ($P > 0.05$). Omission of the primary antibodies resulted in less than 2% of the labeling obtained with primary antibodies against GLUT4.

Neither Insulin Nor Muscle Contractions Affect Accessibility of GLUT4 NH_2- or COOH-terminal Epitopes

It has been suggested that GLUT4 COOH-terminal epitopes are masked in basal fibers but become unmasked after stimulation with insulin (Wang et al., 1996). To measure the total amount of binding of anti-GLUT4 antibodies to the fibers, we used an ^{125}I-labeled secondary antibody. Single fibers were labeled with either the anti–COOH-terminal GLUT4 antibody or with an anti–NH_2-terminal GLUT4 antibody or with anti–caveolin-3 used as an independent marker of the muscle cell surface to correct for differences in fiber and sarcomere length. The number of COOH-terminal and NH_2-terminal GLUT4 epitopes accessible to antibody binding is unaffected by stimulation with either insulin, muscle contractions or both stimuli combined (Fig. 5). The anti–NH_2-terminal GLUT4 antibody (Kahn et al., 1991; Smith et al., 1991) was also used to stain fibers for both LM and EM (Ploug and Ralston, 1998). In both cases, the pattern observed in basal fibers was similar to that observed with the COOH-terminal anti-GLUT4. Therefore, our results do not support the concept of GLUT4 epitope masking and thereby
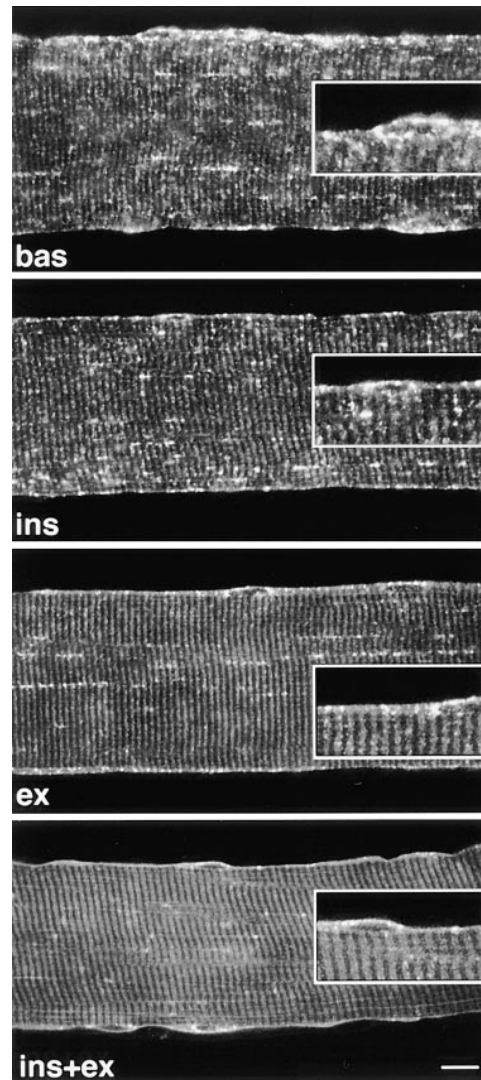
Figure 6. Confocal images reveal translocation of GLUT4 to the plasma membrane and T tubules of stimulated fibers. Teased single fibers from basal (*bas*), insulin- (*ins*), contraction- (*ex*), and insulin- and contraction-stimulated muscles (*ins+ex*) were permeabilized and stained with rabbit anti-GLUT4 followed by biotin-conjugated anti-rabbit IgG and FITC-labeled streptavidin. Confocal images (12 for each condition) were collected from a plane close to the center of the fibers, as described in the Methods section. Notice the appearance of a continuous plasma membrane staining and of cross-striations, especially noticeable in insulin- and contraction-stimulated fibers (*ins+ex*), and the progressive disappearance of the strong dotted pattern when going from basal fibers to fibers stimulated with either or both stimuli. *Insets*, an enlarged view of the fiber surface. Bar, 5 μm.

validate the use of anti–COOH-terminal GLUT4 antibodies that were used throughout the present work.

Stimulation with Insulin and Contractions Result in Additive Translocation of GLUT4 to Both Plasma Membrane and T Tubules

To get a global view of the changes in GLUT4 distribution after stimulation by insulin, contractions, or both stimuli

combined, recordings were done from random areas of single fibers by confocal microscopy. Three changes are striking (Fig. 6) when comparing representative images of basal and stimulated muscle: (*a*) the appearance of a continuous plasma membrane staining, (*b*) the appearance of cross-striations, and (*c*) a decrease in intensity of the GLUT4 aggregates. The periodicity of the cross-striations corresponds to the periodicity of the sarcomeres. At high magnification, the cross-striations appear as doublets (Fig. 6, *insets*) separated by a thin black line, which at the EM level corresponds to the Z line (see below). The changes are most evident in fibers from muscles stimulated by both insulin and contractions (Fig. 6, *ins+ex*), with individual stimuli alone (Fig. 6, *ins* and *ex*) producing smaller changes. Therefore, the confocal images support the notion that, after stimulation by either insulin or contractions, GLUT4 aggregates become attenuated and in part translocated to the plasma membrane and to internal membranes, presumably the T tubules, resulting in a homogeneous staining of the whole external surface of the muscle fiber. This is confirmed by immunogold EM (Fig. 7) which shows that insulin and muscle contractions both induce a translocation of GLUT4 to the two major domains of the surface membrane, i.e., the plasma membrane (Fig. 7, *a* and *b*) and the T tubules (Fig. 7, *c–g*). Golgi complexes (Fig. 7 *i*) are labeled, but less heavily than in basal fibers, and multivesicular bodies show less labeling as well (Fig. 7 *h*). The staining intensity of the plasma membrane appears somewhat variable when following long stretches of intact membrane. However, we do not detect any specialized microdomains, within the span of several sarcomeres, that could function as specific target areas. Quantitative analysis (Table I) shows that insulin increases GLUT4 labeling on the plasma membrane approximately sevenfold, contractions ninefold, and the two stimuli combined 14-fold, demonstrating a roughly additive effect of the two stimuli. Similarly, insulin increases GLUT4 labeling on the T tubule membrane approximately 15-fold, contractions 20-fold, and the two stimuli combined 30-fold, again a roughly additive effect. It should also be noted that the density of GLUT4 labeling (grains/10 μm membrane) along the plasma membrane is quite similar to that along the T tubules (Table I). The degree of labeling of T tubules was also expressed in an alternative way, in order to take advantage of the large number of T tubules that are sectioned transversely (∼85% of the total number of encountered T tubules). The labeling of these cross-sections is all or none: they are labeled with either one grain or no grain. It is evident that the probability that any given T tubule will in fact be labeled is proportional to the labeling density of the T tubule. We have therefore also calculated the effect of stimulation on T tubule labeling expressed as percent of labeled sections of T tubules, including both cross- and longitudinally sectioned T tubules (Table I). The increase after stimulation observed for these counts is slightly larger but of the same order of magnitude as the labeling density measured on longitudinally sectioned T tubules, and the degree of additivity is the same.

Immunocytochemical labeling of teased fibers requires permeabilization. To rule out permeabilization-related artefacts we also stained semithin and ultrathin cryosections (Tokuyasu, 1980, 1989) from basal and stimulated muscle (data not shown). Maximum stimulation with insulin and muscle contractions resulted, as observed by LM, in a GLUT4 staining pattern similar to that obtained with confocal microscopy of whole mounts (Fig. 6). Using antibodies or protein A labeled with colloidal gold, even as small as 5 nm, resulted in very little EM labeling but switching to the Fab fragments labeled with 1.4-nm gold clusters considerably increased the labeling efficiency. The results confirmed those obtained by the preembedding technique: in basal fibers GLUT4 was absent from the plasma membrane but was found in tubulovesicular structures close to the plasma membrane. Maximum stimulation with combined insulin and contractions resulted in an 8.6-fold increase in GLUT4 labeling of the plasma membrane (1.3 grains/10 μm in basal fibers compared with 11.2 grains/10 μm after stimulation, based on counting of ∼150 μm of plasma membrane in each condition). The cryosectioning experiments confirm the results obtained by the preembedding technique. However, the morphology of the sections was generally of insufficient quality for the definite identification of GLUT4-labeled internal structures. The addition of low amounts of glutaraldehyde (0.1–0.2%) to the fixative improved the contrast and integrity of the membranes, but severely decreased the labeling efficiency. Thus, with the present experimental system, preembedding labeling seems superior to postembedding labeling.

Diameter of T Tubules Is Not Affected by Stimulation

Wang et al. (1996) recently reported that insulin stimulation of soleus muscle from GLUT4-overexpressing transgenic mice results in a twofold increase in the diameter of the lumen of junctional T tubules. We have measured the diameter of T tubules in fibers from rat soleus muscle fixed either by our normal procedure, or by the fixation procedure of Wang et al. (1996), which includes 0.5% glutaraldehyde. We do not find any significant change ($P > 0.05$) in the diameter of the T tubules in muscle after stimulation with either insulin or contractions (Fig. 8).

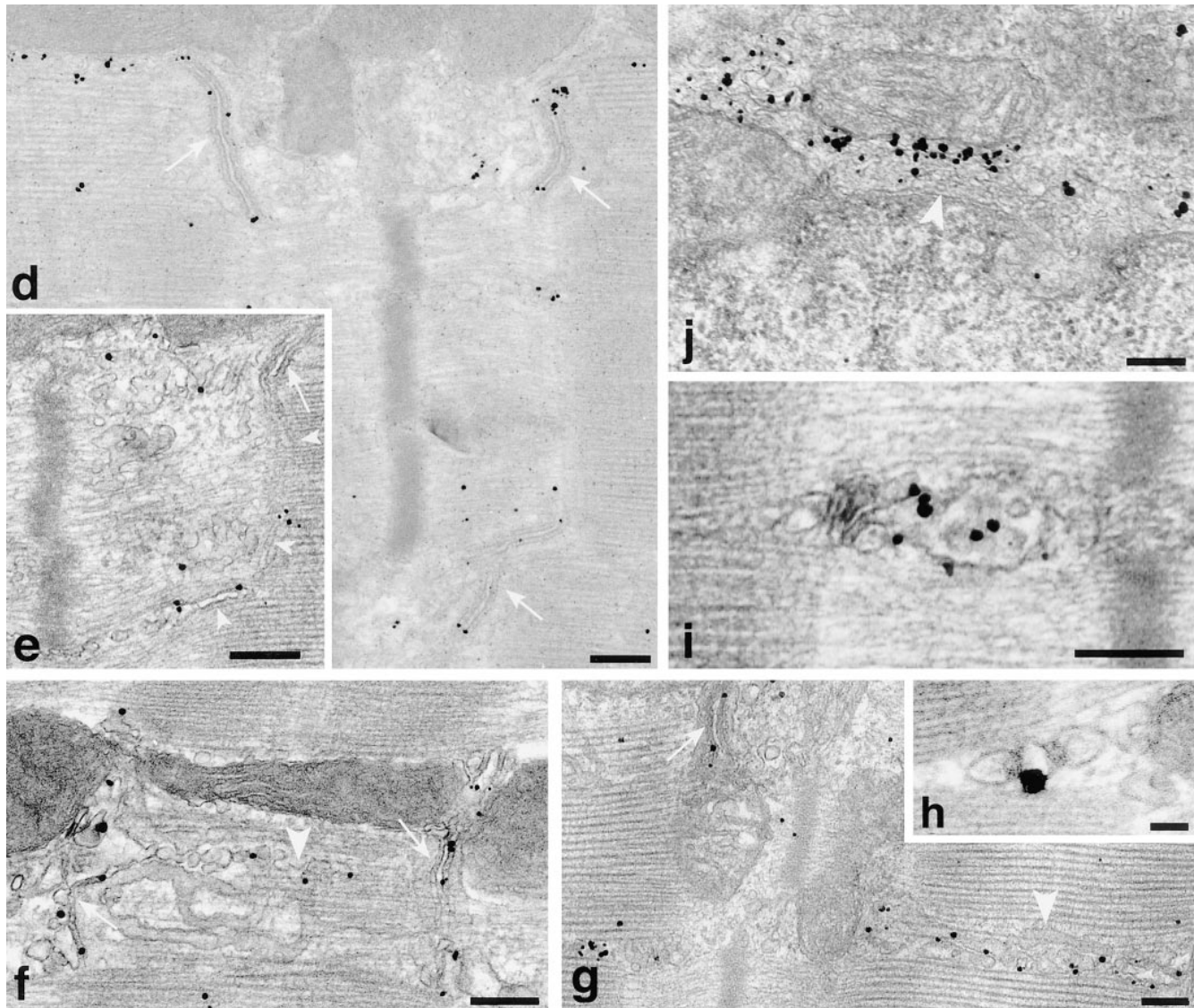### Both Insulin and Contractions Recruit GLUT4 from the Small and Large Depots

To determine which type of GLUT4 depot is recruited by each of the two stimuli, we recorded a large number of z series of confocal images at the surface of fibers from all stimulation conditions, all with the same settings (refer to Materials and Methods). From the projections of the z series we calculated the average pixel density around nuclei. We found it to decrease by ∼30 and 25%, respectively, after insulin and contraction stimulation and by ∼50% after combined stimulation (Table II). A representative projection from each of the four stimulation conditions is shown in Fig. 9. Insulin and contractions decrease the GLUT4 staining of both large and small depots demonstrating that each of the two stimuli recruit transporters from both categories of storage sites. At the EM level, we find that the decrease in the staining of the large structures is partial, whereas it is all or none for the small GLUT4 clusters, whose number is decreased (Table II).
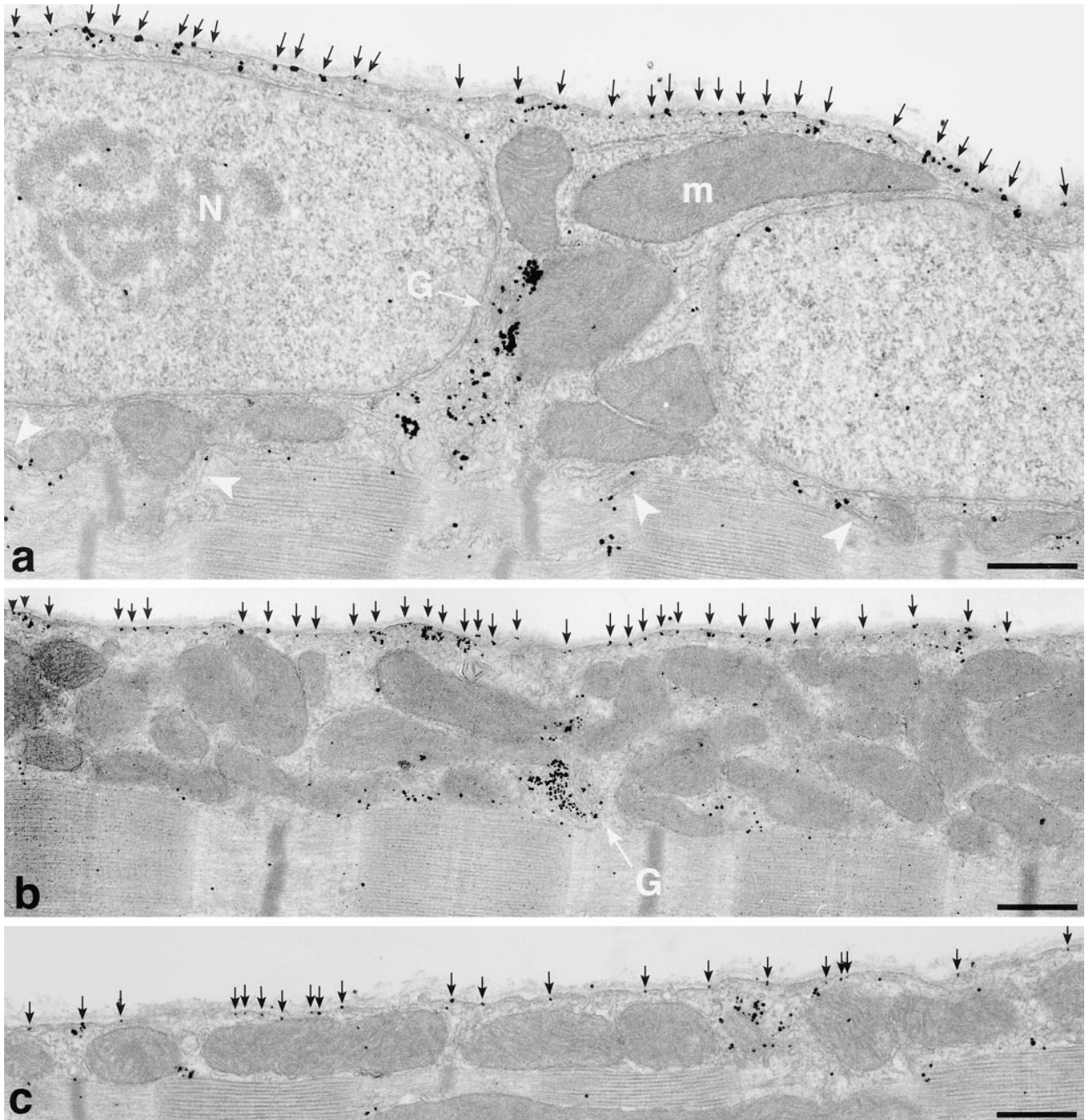
Small GLUT4 Clusters Can Be Subdivided into TfR-negative Elements, Which Are Recruited by Insulin, and TfR-positive Elements, Which Are Recruited by Contractions

The association of GLUT4 with multivesicular bodies (refer to Fig. 4) suggests that part of GLUT4 is localized to the endosomal system. This is in line with recent subcellular fractionation findings in 3T3-L1 adipocytes (Livingstone et al., 1996; Martin et al., 1996) and skeletal muscle (Aledo et al., 1997; Sevilla et al., 1997), which also further suggested that insulin primarily recruits GLUT4 from a nonendosomal compartment. To analyze this at the morphological level, we double stained fibers for GLUT4 and

TfR (Fig. 10). TfR staining, like GLUT4, shows both large perinuclear and smaller elements. When the two images are superimposed, there is a partial overlap of the staining in the perinuclear region, which is exaggerated due to the recording parameters, which were optimized for observation of the smaller, dimmer elements. There is also some overlap in the small GLUT4-containing elements, both at the surface of the fibers (Fig. 10, *left panels*) and in the myofibrillar core (Fig. 10, *right panels*). When the small elements that are above a nucleus are enlarged in cartoon form in Fig. 10 (*bottom panel*), it can be seen more easily that a major part, though not all of the overlap occurs in larger irregular structures. In contrast, GLUT4-positive/

Figure 7. Translocation of GLUT4 in stimulated fibers observed by preembedding immunogold electron microscopy. (*a*) Overview of a fiber that has been maximally stimulated with both insulin and contractions, showing two nuclei (*N*) and several mitochondria (*m*). The plasma membrane contains numerous single grains (*black arrows*) and the T tubules of several triad junctions also appear labeled (*white arrowheads*). GLUT4 labeling is also found at the pole of one of the nuclei, in the Golgi complex region (*G*). (*b*) Despite the heavy labeling of the plasma membrane (*black arrows*) in a fiber from contraction-stimulated muscle, the Golgi stack (*G*) still has fairly dense polarized GLUT4 labeling. (*c*) Overview of a fiber from an insulin-stimulated muscle showing dense labeling of the plasma membrane (*black arrows*). (*d–h*) Labeling of junctional T tubules (*white arrows*) in fibers from exercise- (*d* and *f*) or insulin and exercise-stimulated (*e* and *g*) muscle. In *e*, the nonjunctional part of a T tubule leaving a triad can be seen (*white arrowheads*) coursing between the myofibrils. The labeling of apparently fenestrated SR (*f* and *g, white arrowheads*) is mostly in the form of single grains and not of clusters of grains as seen in nonstimulated fibers. (*h*) Labeling of the T tubule in a cross-sectioned triad in a fiber from insulin-stimulated muscle. (*i*) Labeling of an endosome in the myofibrillar core of an insulin-stimulated fiber. (*j*) The labeling of the TGN area in an insulin and exercise-stimulated fiber appears lighter than in basal fibers. Bars: (*a–c*) 0.5 μm; (*d–g, i,* and *j*) 0.2 μm; (*h*) 0.05 μm.

TfR-negative elements generally appear smaller and more dot-like. Double staining of fibers from insulin- and contraction-stimulated muscle (Fig. 11) shows that the small dot-like GLUT4-positive/TfR-negative elements are very much decreased after insulin stimulation, whereas the larger irregular GLUT4-positive/TfR-positive elements have nearly all gone from contraction-stimulated fibers. GLUT4/TfR colocalization was quantitated (refer to Materials and Methods). We find that 52 ± 4% (mean ± SE, $n = 8$) of GLUT4 staining, in basal muscle, overlaps with TfR staining. This fraction increases significantly to 69 ± 4% after insulin stimulation ($n = 8$; $P < 0.05$) and decreases to 39 ± 4% after contractions ($n = 8$; $P < 0.05$). At the EM level, TfR is found in the TGN region, associated with multivesicular bodies, and in small clusters underneath the plasma membrane and close to the T tubules (Fig. 12).

The impression from Fig. 11 that only contractions re-

Table I. Quantitation of the Effects of Insulin and Muscle Contractions on GLUT4 Labeling in the Surface Membrane

	Basal	Insulin	Contractions	Insulin + contractions
Plasma membrane*	1.7 ± 0.3	12.6 ± 0.7	14.7 ± 6.0	23.1 ± 3.0
	(5/1409 μm)	(4/929 μm)	(4/1473 μm)	(5/1634 μm)
Increase over basal	× 1	× 7	× 9	× 14
T tubules (longitudinally sectioned)‡	0.6 ± 0.7	8.7 ± 0.6	13.5 ± 5.1	18.2 ± 3.8
	(3/82/34 μm)	(3/119/60 μm)	(3/161/85 μm)	(3/198/74 μm)
Increase over basal	× 1	× 15	× 23	× 30
T tubules (cross-sectioned plus longitudinally sectioned)§	0.8 ± 0.7	19.4 ± 1.2	23.3 ± 6.4	33.4 ± 2.6
	(5/1316)	(4/1010)	(4/1616)	(5/1276)
Increase over basal	× 1	× 24	× 29	× 42

Fibers from each of the four experimental groups were labeled with anti-GLUT4 and processed for immunogold electron microscopy. Silver-enhanced gold grains were counted from longitudinal sections. All results are given as means ± SEM. Numbers in parentheses represent the number of independent experiments counted, followed for rows *1* and *2* by the total length of membrane counted (in μm), and for rows *2* and *3* by the number of triads counted.

*Number of grains/10 μm of plasma membrane. The background labeling in the absence of primary antibody was 2.8 ± 0.2 grains/10 μm and has been subtracted from the presented data.

‡Number of grains/10 μm of longitudinally sectioned junctional T tubule membrane. The background labeling in the absence of primary antibody was 1.2 ± 0.7 grains/10 μm and has been subtracted from the presented data.

§Percent of junctional T tubules labeled, including both cross- and longitudinally sectioned T tubules. In the absence of primary antibody 1.4 ± 0.4% of all triads were labeled. This has been subtracted from the presented data. Cross-sectioned T tubules represent ∼85% of the total number of encountered T tubules.

cruit TfR-positive elements, is confirmed by subcellular fractionation (Fig. 13). A crude microsomal fraction was separated on a density gradient. Four fractions (F1–F4) were collected. They were characterized by immunoblotting with antibodies to the Na^+/K^+-ATPase and the dihydropyridine receptor as markers of the plasma membrane and T tubules, respectively, and with antibodies to GLUT4 and TfR. F1 and F2 account for most of the plasma membrane and T tubule markers (F1 contains ∼60% of the total amount of Na^+/K^+-ATPase α_1 subunit and F2, ∼30%; each contains ∼40% of the dihydropyridine receptor), but

F2 is a mixed fraction since it also contains a large fraction of GLUT4 in basal muscle (Fig. 13). F3 and F4 contain primarily internal membranes (∼30% of the SR Ca^{2+}-ATPase [SERCA 1] is found in F3 and ∼60% in F4). Insulin and contractions cause an additive translocation of GLUT4 from F3 and F4 to F1. Since F2 contains both intracellular GLUT4 vesicles and surface membranes, no net change of total GLUT4 content is detected in this fraction. Interestingly, only contractions cause a substantial translocation of TfR from F2 and F3 to F1, whereas insulin affects the distribution of TfR only slightly, or not at all. A
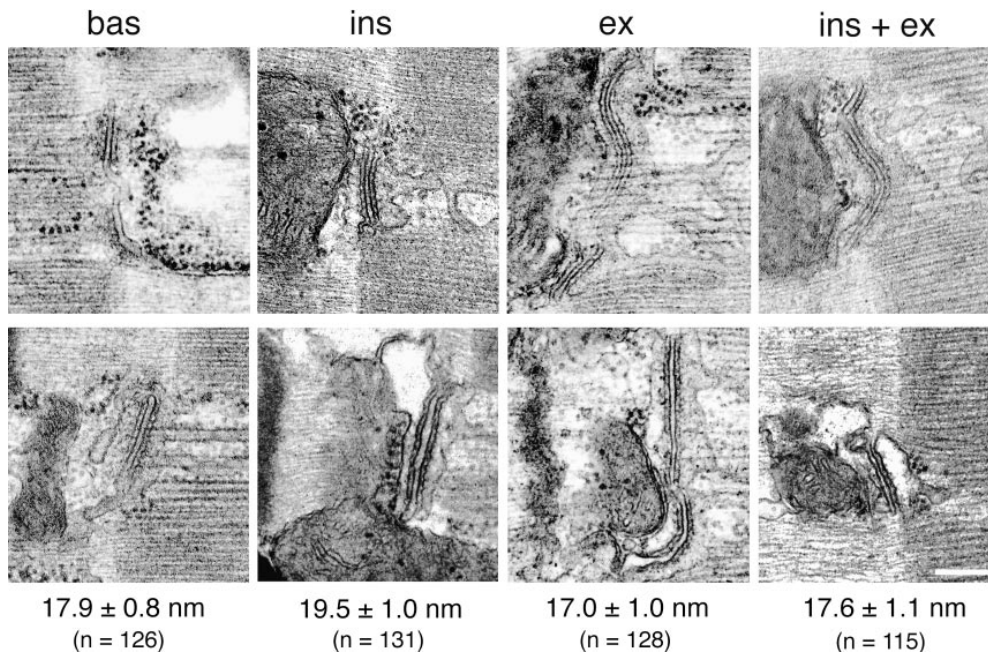

bas   ins   ex   ins + ex

17.9 ± 0.8 nm   19.5 ± 1.0 nm   17.0 ± 1.0 nm   17.6 ± 1.1 nm
(n = 126)   (n = 131)   (n = 128)   (n = 115)

Figure 8. Stimulation does not affect the diameter of T tubules. Muscles from basal and stimulated rats were fixed by perfusion with 3% formaldehyde + 0.5% glutaraldehyde (*top*) or with 2% formaldehyde alone (*bottom*), embedded and sectioned (refer to Materials and Methods). Under the microscope, the A–I junction was followed until a longitudinally sectioned triad junction was encountered. A photograph was taken, the grid was then shifted by a few sarcomeres, and then the search resumed. After five photographs another fiber was selected, etc. The diameter of the T tubules was measured from photographs taken at a primary magnification of 25,000, with a 7× magnifying glass 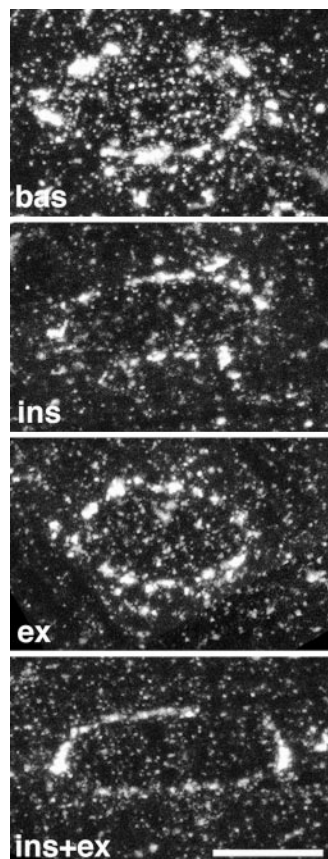equipped with a measuring scale. The photographs show a typical T tubule for each condition. For each of the fixation procedures, T tubules were sampled from two independent experiments, each including the four stimulation states. Two-way ANOVA did not detect any interaction between fixation conditions and T tubule diameter, nor any effect of stimulation on T tubule diameter ($P > 0.05$). Therefore, measurements obtained by the two fixation procedures were pooled. The average diameter (mean ± SEM) as well as the total number of T tubules measured (*n*) are shown for each condition. Bar, 0.2 μm.

possible explanation of the fact that TfR but not GLUT4 is reduced in F2 after contractions is that TfR-positive/GLUT4-negative elements in F2 also translocate to F1. Thus, in agreement with the morphological observations, subcellular fractionation independently suggests that only one stimulus, muscle contractions, causes a substantial translocation of TfR to the cell surface.

Discussion

The methodological approach used in this study sets it apart from other studies in the field. The use of whole mounts of muscle fibers in immunofluorescence and the preembedding technique used for immunogold EM are especially suited to the unique geometry of muscle fibers. In contrast, we find that the EM postembedding technique that has been so elegantly used in studies of GLUT4 in adipose cells (Slot et al., 1991*a*) and cardiac muscle (Slot et al., 1991*b*, 1997), gives a very poor labeling efficiency in skeletal muscle. Even with a very small 1.4-nm gold cluster covalently coupled to a Fab fragment, we find that the labeling efficiency is less than half of that obtained by preembedding labeling. The reason why the postembedding labeling efficiency of GLUT4 appears to be higher on sections from fat and heart (Slot et al., 1991*a*,*b*, 1997) than from skeletal muscle is not clear.

It has been firmly established that the increase in glucose uptake after insulin stimulation of adipose cells and of cardiac muscle results from the exocytosis-like movement of GLUT4-containing vesicles from intracellular sites to the cell surface. By analogy, it then appears likely

Table II. Quantitation of the Effects of Insulin and Muscle Contractions on GLUT4 Intracellular Depots

|		Basal	Insulin	Contraction	Insulin + contractions
LM	Average pixel density around nuclei*	100.0 ± 5.7 (1/42)	68.9 ± 4.1 (1/27)	74.2 ± 4.5 (1/31)	51.6 ± 3.7 (1/39)
EM	TGN‡	67 ± 18 (2/20)	56 ± 14 (2/13)	49 ± 2 (2/14)	36 ± 10 (2/26)
EM	Subsarcolemmal cytoplasm§	38.6 ± 7.1	34.3 ± 5.7	28.6 ± 2.9	15.7 ± 7.1
	I band	16.1 ± 0.0	9.1 ± 2.7	9.1 ± 1.6	5.4 ± 0.0
	A band	4.5 ± 0.3 (2/402)	2.4 ± 0.3 (2/209)	1.4 ± 0.7 (2/288)	0.9 ± 0.3 (2/150)

Fibers from each of the four experimental groups were labeled with anti-GLUT4 antibody and processed for either immunofluorescence (*LM*) or immunogold electron microscopy (*EM*). All results are given as mean ± SEM. The numbers in parentheses represent the number of independent experiments followed by the number of organelles or vesicles counted. Since nonspecific labeling at the EM level in the absence of primary antibody only consists of mostly single grains (never more than two together) and the average size of the small GLUT4 depots consisted of on average eight grains, no background correction has been done on these data.
*Z series of confocal images at the surface of fibers were recorded at high magnification (refer to Materials and Methods). The average pixel density around nuclei (as shown in Fig. 9), using maximum projections, was calculated.
‡Number of grains associated with each identifiable stack of Golgi cisternae, primarily located in the TGN.
§Number of small GLUT4 depots per 100 μm^2 in the subsarcolemmal cytoplasm (defined as the region between the plasma membrane and the myofibrils), and in the I and A bands.

Figure 9. GLUT4 is recruited from both large and small depots after stimulation. z series of four confocal images starting at the surface of the fibers, with successive images separated by 0.7 μm were recorded from 10–15 different fibers for each of the four conditions (*bas*, *ins*, *ex*, and *ins+ex*). Projections of the series were calculated. Shown here is one representative projection for each condition. Note that the intensity of the perinuclear staining and the density of the small depots both decrease with stimulation, with single stimuli causing a decrease intermediate to that caused by combined stimulation. Bar, 5 μm.

that this process, known as translocation should take place in all GLUT4-containing tissues. However, a recent study claimed that insulin acts primarily by unmasking a COOH-terminal epitope of GLUT4 transporters which constitutively reside in the plasma membrane and T tubules of muscle but are not accessible in basal fibers (Wang et al., 1996). This implies that the total number of GLUT4 COOH-terminal epitopes increases upon stimulation. However, when we measure the total number of epitopes accessible to anti-GLUT4 antibodies raised against both NH_2- and COOH-terminal epitopes, we find no difference between basal and stimulated fibers (refer to Fig. 5). Therefore, the increased labeling of the plasma membrane and T tubules that we observe after stimulation (refer to Table I and Figs. 6 and 7) clearly demonstrates that both insulin and muscle contractions cause a large translocation of GLUT4 from intracellular storage sites. Our results differ from those of previous immunocytochemical studies of skeletal muscle that reported labeling of the plasma membrane but not of the T tubules (Rodnick et al., 1992), or of the T tubules but not of the plasma membrane (Friedman et al., 1991; Dohm et al., 1993) after stimulation with insulin. However, our findings are in line with those of Slot et al. (1991), who found labeling of both the plasma membrane and T tubules of cardiac myocytes after insulin stimulation. They also found that the labeling efficiency, using an anti-GLUT4 COOH-terminal antibody, was the same in basal and insulin-stimulated cells, which is in agreement with the present observations in skeletal muscle. The discrepancies between the present study and previous studies in skeletal muscle (Friedman et al., 1991; Rodnick et al., 1992; Dohm et al., 1993) is probably due to the fact that postembedding labeling was used in the cited studies com-
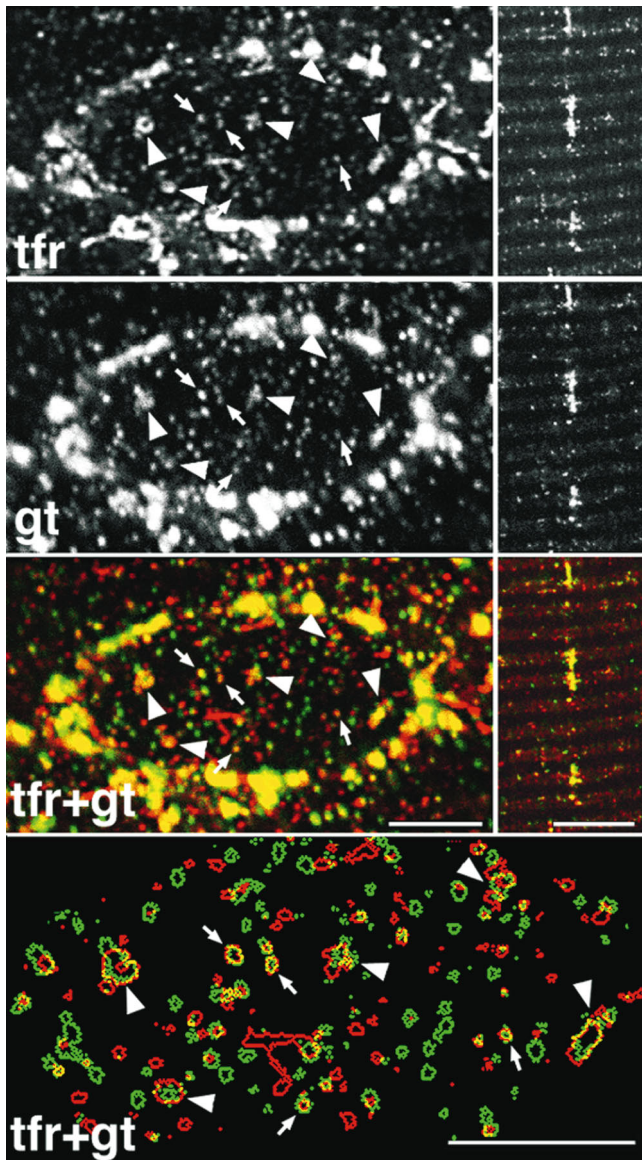
Figure 10. Partial association of GLUT4 and transferrin receptor-containing structures at the surface and in the core of basal fibers. Single basal fibers were stained simultaneously with an antibody to the transferrin receptor (*tfr*) followed by a Texas red–conjugated secondary antibody, and to GLUT4 (*gt*) followed by a fluorescein-conjugated secondary antibody. Single confocal images were recorded, separately for each fluorophore, from the surface (*left panels*) or the core (*right panels*) of the fibers. The core views were rotated by 90° compared with surface views. In the large depots of the perinuclear belt, there is a large degree of overlapping (*yellow*) which is exaggerated by saturation of the image. In the smaller depots that are encircled by this belt, there is much less overlap. The small depots are shown, enlarged, in the bottom panel which displays their computer-drawn contours. Most of the depots are small and round. Only a small fraction of these overlap (*arrows*). Some depots are larger and irregularly shaped. They show a large degree of overlap (*arrowheads*). Notice, however, that the *green* and *red* contours are differently shaped. Bars, 5 μm.
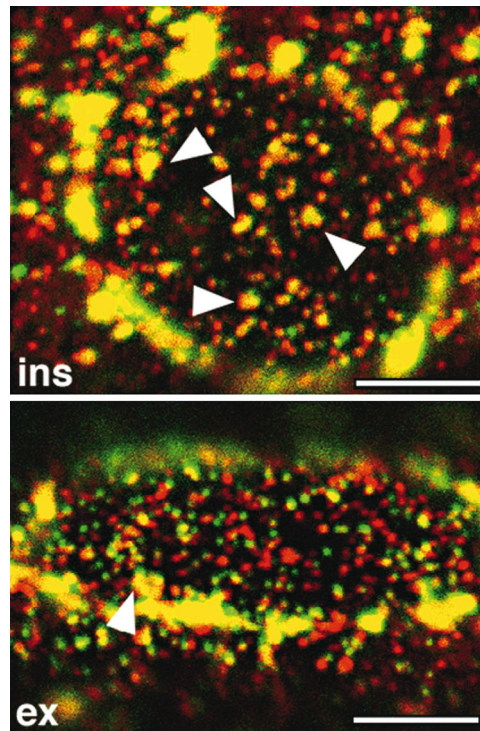
Figure 11. Association of GLUT4 and TfR is increased by insulin but decreased by contractions. Single fibers from insulin- or contraction-stimulated muscle were stained and observed as described in the legend for Fig. 10. Note the increased overlap of the two stainings in insulin-stimulated fibers and the decreased overlap in contraction-stimulated fibers compared with basal fibers (refer to Fig. 10), suggesting that GLUT4$^+$/TfR$^-$ elements are recruited by insulin and GLUT4$^+$/TfR$^+$ elements are recruited by contractions. Bars, 5 μm.
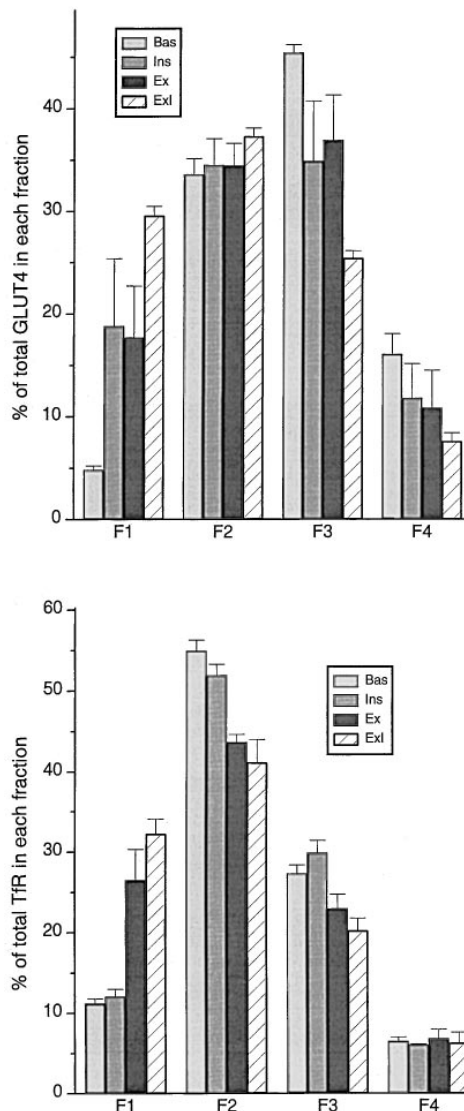
pared with the present preembedding approach. The present study is the first to address by immunocytochemical techniques the effect of contractions on GLUT4 subcellular distribution. However, by biochemical techniques both stimuli have been shown to increase GLUT4 content in membrane fractions enriched in either of the two surface membrane domains (Douen et al., 1990; Marette et al., 1992; Munoz et al., 1995; Roy and Marette, 1996). The effects of the two stimuli on translocation of GLUT4 are additive (refer to Table II), as are their effects on glucose transport (Nesher et al., 1985; Ploug et al., 1987; Constable et al., 1988). The magnitude of the translocation (refer to Table I) is sufficient to account for the increase in glucose transport, which is typically in the order of 3–30 fold depending on muscle fiber type (James et al., 1985; Ploug et al., 1987; Henriksen et al., 1990). It is also consistent with results obtained from photolabeling experiments in skeletal muscle (Wilson and Cushman, 1994; Lund et al., 1995) and adipose cells (Holman and Cushman, 1994). Compared with other muscles the soleus used in the present study has a rather large increase in transport after stimulation.

In the soleus muscle, the surface area of the T tubules is similar to that of the plasma membrane (Davey and Wong, 1980; Cullen et al., 1984), and since we find that the labeling density of the two surface domains is quite similar (re-
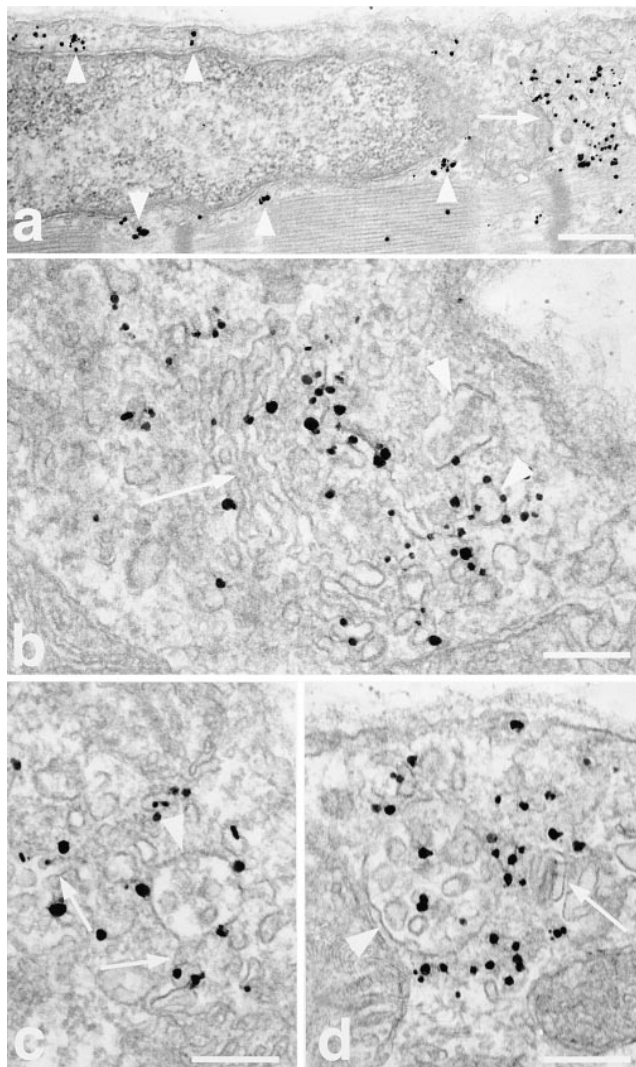
Figure 12. Immunogold EM localization of the TfR in basal fibers. Single fibers were stained for TfR and embedded in epoxy resin as described in Materials and Methods. (*a*) Low magnification overview showing an area around a nucleus near the plasma membrane. TfR is present in large aggregates in the area of the Golgi complex (*arrow*) and in smaller aggregates all around the nucleus (*arrowheads*) in a pattern that resembles that seen for GLUT4 in Fig. 4. (*b*) A stack of Golgi cisternae (*arrow*) showing TfR labeling, both in the cisternae and in vesicles of different sizes around the cisternae (*arrowheads*). (*c* and *d*) Labeling is often seen associated with multivesicular bodies (*arrowheads*) of different sizes. In *c,* the labeling seems excluded from the internal structures whereas in *d* they are labeled. Note also a network of labeled, tubulovesicular structures (*arrows*) around the multivesicular bodies. Bars: (*a*) 0.5 μm; (*b–d*) 0.2 μm.

Figure 13. Subcellular membrane fractionation shows that TfR only translocates in response to contractions. Four membrane fractions (F1–F4) were prepared from rat hindleg muscles from four group of rats (*Bas*, *Ins*, *Ex*, and *ExI*). 5 μg of protein from each fraction were separated by SDS-PAGE and analysed by Western blotting using antibodies against GLUT4 and TfR followed by ^{125}I-labeled secondary antibody. The bands were quantitated with a PhosphorImager and the contribution of each band to the sum of bands in the four fractions is expressed in percentages. Values are means ± SEM of 3–5 independent experiments. Insulin and contractions result in an additive translocation of GLUT4 to F1 (enriched in plasma membranes and T tubules), from F3 and F4 (enriched in intracellular membranes). In contrast, only contractions result in translocation of TfR from F2 and F3 to F1. TfR-positive vesicles recruited from F2 are probably GLUT4 negative, since the GLUT4 content in F2 is unaffected by stimulation, whereas those recruited from F3 are probably GLUT4 positive.

fer to Table I), then the plasma membrane and the T tubules must contribute equally to the overall glucose uptake. This is very different from the claim that the T tubules should contribute nine times more to glucose uptake than the plasma membrane (Wang et al., 1996). This was based on average T tubule diameters at least twice those measured by us (refer to Fig. 8) and on a further 50% increase in this diameter after insulin stimulation. We do not find any effect of stimulation on T tubule diameters,

whether using our usual fixation conditions or those used by Wang et al. (1996). Species differences may account for this discrepancy since their work was carried out on mice; in addition, overexpression of GLUT4 in the transgenic

animals studied by Wang et al. (1996) may affect muscle morphology. Within the plasma membrane or the T tubules, we have not observed the targeting of GLUT4 to recognizable microdomains, such as the costameric region of the plasma membrane (Munoz et al., 1995). However, it sometimes appears that sections of the plasma membrane close to intracellular GLUT4 depots are more heavily labeled after stimulation than more distant areas of the surface membrane.

Muscle cells are very large, multinucleated cells. A single soleus fiber in an adult rat is ~1.5 cm in length, 30–50 μm in diameter, and contains hundreds of nuclei that are located just underneath the plasma membrane and which are separated from each other by large distances. How is GLUT4 distributed in such a cell? Is it uniformly distributed along the fiber, or localized to specific areas? Is it close to the fiber surface and therefore to the blood vessels that irrigate the muscle, or is it also found in the core of the fibers? By examining muscle fibers as whole mounts, we find that GLUT4, in basal fibers, is distributed all along the muscle fibers, and is present both at the surface (68% of total GLUT4) and in the core (32%) of the fibers. We also find (refer to Fig. 2) that the nuclei are displaced by and aligned with the many blood vessels that course along the fiber surface, thereby placing a large fraction of GLUT4 close to the source of glucose and obviating the need for diffusion over long distances.

The original observation in brown adipose cells and cardiac myocytes that the main intracellular storage sites for GLUT4 in basal cells include the TGN region and tubulovesicular structures clustered in the cytoplasm, often just beneath the cell surface (Slot et al., 1991a,b), was soon followed by similar observations in skeletal muscle (Bornemann et al., 1992; Rodnick, 1992; Takata et al., 1992). In the present study we have extended and quantitated these observations. By light microscopy we find GLUT4 to be in two kinds of depots: large elements, which include ~23% of total GLUT4, surround the nuclei and form long rows between the nuclei and in the core of the fibers; and small elements, which comprise ~77% of total GLUT4, are found throughout the fibers. The large depots represent tubulovesicular elements in the TGN region. Our definition of the TGN is purely morphological: it includes the last cisterna(e) of the Golgi complex and tubulovesicular structures beyond (Griffiths and Simons, 1986; Mellman and Simons, 1992). If other criteria are used to define the TGN, for example, colocalization with the protein TGN38 (Banting and Ponnambalam, 1997), the assignation of the large depots to the TGN is much less certain. Indeed, GLUT4 appears only partially colocalized with TGN38 in LM (this study), in agreement with subcellular fractionation studies which have found very little or no colocalization (Martin et al., 1994; Sevilla et al., 1997). Immunogold EM observations of TGN38 in soleus fibers show most grains to be in the Golgi cisternae (manuscript in preparation), which contain relatively little GLUT4 (refer to Fig. 4). TGN38 was previously believed to be absent from skeletal muscle (Antony et al., 1995). Finally, in cultured myotubes, GLUT4 also appears to accumulate in the TGN, but its pattern after treatment of the cultures with brefeldin A is completely different from that of TGN38 (Ralston and Ploug, 1996a). Since it is well known that the shape and size of the TGN vary between cells and depend on their secretory capacity (Clermont et al., 1995), it is conceivable that muscle has developed a specialized subcompartment of the TGN dedicated to GLUT4 storage (Rahkila et al., 1998).

The large depots of GLUT4 are also associated with multivesicular bodies that are found so close to the Golgi complex that it is often difficult to distinguish, even in electron micrographs, whether high densities of GLUT4 grains are associated with one or the other. Muscle nuclei are surrounded by a dense belt of subcellular organelles. Since immunogold EM shows the multivesicular bodies found in this belt to contain TfR (refer to Fig. 12), they must be considered as early endosomes (Mukherjee et al., 1997). The association of Golgi complexes and TfR-positive endosomes is also seen in the long rows of staining found along the surface and in the core of the fibers (refer to Fig. 10).

The small GLUT4 depots are seen throughout the fibers. They are not associated with the Golgi complex but ~52% appear to be associated with TfR-positive endosomes (refer to Fig. 10). The TfR-negative/GLUT4-positive elements are rather small, round, and quite uniform in size. In contrast the TfR-positive/GLUT4-positive structures are somewhat larger and more irregular in shape (refer to Fig. 10). Thus, the small GLUT4 depots fall into two categories based on TfR content and somewhat more arbitrarily on size and shape. Since, in this work, the degree of GLUT4 and TfR association was measured from LM images, we cannot affirm that all of it represents true colocalization of the two markers within vesicles. In addition, because of the thresholding procedure used in the calculations (refer to Materials and Methods), the contribution of vesicles that contain little GLUT4 is exaggerated, probably inflating the percent of colocalization in all conditions. Nevertheless, our numbers are not very far from some of those obtained by others. That a substantial fraction of GLUT4 in mature skeletal muscle is actually localized to the same structures as the TfR was recently shown by immunopurification of GLUT4 vesicles (Aledo et al., 1997). This is also consistent with findings in 3T3-L1 adipocytes, in which ~40% of total cellular GLUT4 content colocalize with the TfR (Livingstone et al., 1996; Martin et al., 1996). In contrast, in studies of freshly isolated rat adipocytes (Malide et al., 1997) and brown adipose tissue (Slot et al., 1991a), and in our own work with C2 myotubes (Ralston and Ploug, 1996a), only a small fraction of GLUT4 appears to be associated with endosomes. It is thus clear that the fraction of GLUT4 that resides in the endosomal recycling system is cell type-specific and depends on the level of differentiation.

Results from light and electron microscopy (refer to Figs. 7 and 9, and Table II) demonstrate that both small and large depots serve as GLUT4 donor sites in stimulated fibers. Stimulation with insulin, contractions, or both stimuli combined, result in a decrease in the size of the large depots, as would befit large tubulovesicular assemblies such as the TGN, which function as a source of vesicles generated by budding (Griffiths and Simons, 1986). Whether these vesicles spend enough time while traveling to the surface membrane to appear as the small GLUT4 depots is currently unknown. Recent studies of the vesicu-

lar stomatitis virus G protein in cultured myotubes (Rahkila et al., 1998) suggest that this is at least possible. After combined stimulation with insulin and contractions, the small depots, which at the EM level appear rather uniform in size and frequently show a circular shape, decrease in number by two- to fivefold, whereas their size is not affected. This is consistent with the small depots representing vesicles which translocate as a unit to the surface membrane. Double labeling for TfR and GLUT4 at the light microscopy level reveals an increased association of the two proteins after insulin stimulation and a decreased association after contractions (refer to Figs. 10 and 11). This indicates that insulin primarily recruits GLUT4-positive/TfR-negative vesicles, whereas contractions primarily recruit GLUT4-positive/TfR-positive vesicles. This is consistent with recent biochemical experiments in skeletal muscle, in which insulin recruited GLUT4 from a pool of nonendosomal associated intracellular GLUT4 vesicles (Aledo et al., 1997; Sevilla et al., 1997). In addition, our own subcellular fractionation experiments (refer to Fig. 13) demonstrate that insulin stimulation results in translocation of GLUT4 with a minimal effect, if any effect at all, on TfR. In contrast, contractions result in a substantial translocation of both GLUT4 and TfR. The notion that insulin and contractions recruit GLUT4 from different intracellular pools has been supported experimentally for several years (Douen et al., 1990; Coderre et al., 1995). However, the present study for the first time visualizes these two pools and demonstrates that the contraction-sensitive pool is part of the endosomal recycling system.

We also find GLUT4 in what appears to be the SR, in agreement with Wang et al. (1996). Interestingly, glycolytic enzymes have recently been shown to be associated with the SR at the ultrastructural level (Xu and Becker, 1998). However, a definite conclusion must await double labeling with SR markers at both the LM and EM level. Although a direct trafficking route between the SR and the cell surface has not been demonstrated, it does not appear unlikely, since the vesicular stomatitis virus glycoprotein traffics between the SR, Golgi complexes, and T tubule membranes (Rahkila et al., 1996).

In conclusion, we have morphologically identified two populations of intracellular GLUT4 vesicles, which are differentially recruited by insulin and muscle contractions. Consistent with this, we have shown that the increase in glucose transport that follows insulin and contraction stimulation of skeletal muscle is due to an additive translocation to both the plasma membrane and T tubules. Unmasking of GLUT4 COOH-terminal epitopes and changes in T tubule diameters do not contribute to the increase in transport. Finally, we find that skeletal muscle has evolved a unique distribution of GLUT4 that is suited to the large dimensions of the fibers and to their specific surface membrane organization, and which fulfills the metabolic needs of the contractile apparatus located throughout the core of the fibers.

References

Aledo, J.C., L. Lavoie, A. Volchuk, S.R. Keller, A. Klip, and H.S. Hundal. 1997. Identification and characterization of two distinct intracellular GLUT4 pools in rat skeletal muscle: evidence for an endosomal and an insulin-sensitive GLUT4 compartment. *Biochem. J.* 325:727–732.

Antony, C., M. Huchet, J.P. Changeux, and J. Cartaud. 1995. Developmental regulation of membrane traffic organization during synaptogenesis in mouse diaphragm muscle. *J. Cell Biol.* 130:959–968.

Banting, G., and S. Ponnambalam. 1997. TGN38 and its orthologues: roles in post-TGN vesicle formation and maintenance of TGN morphology. *Biochim. Biophys. Acta.* 1355:209–217.

Bell, G.I., C.F. Burant, J. Takeda, and G.W. Gould. 1993. Structure and function of mammalian facilitative sugar transporters. *J. Biol. Chem.* 268:19161–19164.

Birnbaum, M.J. 1992. The insulin-sensitive glucose transporter. *Int. Rev. Cytol.* 137A:239–297.

Bornemann, A., T. Ploug, and H. Schmalbruch. 1992. Subcellular localization of GLUT4 in nonstimulated and insulin-stimulated soleus muscle of rat. *Diabetes.* 41:215–221.

Clermont, Y., A. Rambourg, and L. Hermo. 1995. Trans-Golgi network (TGN) of different cell types: three-dimensional characteristics and variability. *Anat. Rec.* 242:289–301.

Coderre, L., K.V. Kandror, G. Vallega, and P.F. Pilch. 1995. Identification and characterization of an exercise-sensitive pool of glucose transporters in skeletal muscle. *J. Biol. Chem.* 270:27584–27588.

Constable, S.H., R.J. Favier, G.D. Cartee, D.A. Young, and J.O. Holloszy. 1988. Muscle glucose transport: interactions of in vitro contractions, insulin, and exercise. *J. Appl. Physiol.* 64:2329–2332.

Cullen, J.J., S. Hollingworth, and M.W. Marshall. 1984. A comparative study of the transverse tubular system of the rat extensor digitorum longus and soleus muscles. *J. Anat.* 138:297–308.

Cushman, S.W., and L.J. Wardzala. 1980. Potential mechanism of insulin action on glucose transport in the isolated rat adipose cell. *J. Biol. Chem.* 255:4758–4762.

Davey, D.F., and S.Y.P. Wong. 1980. Morphometric analysis of rat extensor digitorum longus and soleus muscles. *Aust. J. Exp. Biol. Med. Sci.* 58:213–230.

DeFronzo, R.A., R.C. Bonadonna, and E. Ferrannini. 1992. Pathogenesis of NIDDM: A balanced overview. *Diabetes Care.* 15:318–368.

Dohm, G.L., P.L. Dolan, W.R. Frisell, and R.W. Dudek. 1993. Role of transverse tubules in insulin stimulated muscle glucose transport. *J. Cell. Biochem.* 52:1–7.

Douen, A.G., T. Ramlal, S. Rastogi, P.J. Bilan, G.D. Cartee, M. Vranic, J.O. Holloszy, and A. Klip. 1990. Exercise induces recruitment of the "insulin-responsive glucose transporter." Evidence for distinct intracellular insulin- and exercise-recruitable transporter pools in skeletal muscle. *J. Biol. Chem.* 265:13427–13430.

Friedman, J.E., R.W. Dudek, D.S. Whitehead, D.L. Downes, W.R. Frisell, J.F. Caro, and L. Dohm. 1991. Immunolocalization of glucose transporter GLUT4 within human skeletal muscle. *Diabetes.* 40:150–154.

Griffiths, G., and K. Simons. 1986. The trans-Golgi network: sorting at the exit site of the Golgi complex. *Science.* 234:438–443.

Henriksen, E.J., R.E. Bourey, K.J. Rodnick, L. Koranyi, M.A. Permutt, and J.O. Holloszy. 1990. Glucose transporter protein content and glucose transport capacity in rat skeletal muscles. *Am. J. Physiol.* 259:E593–E598.

Holman, G.D., and S.W. Cushman. 1994. Subcellular localization and trafficking of the GLUT4 glucose transporter isoform in insulin-responsive cells. *Bioessays.* 16:753–759.

Horn, M., and G. Banting. 1994. Okadaic acid treatment leads to a fragmentation of the trans-Golgi network and an increase in expression of TGN38 at the cell surface. *Biochem. J.* 301:69–73.

James, D.E., E.W. Kraegen, and D.J. Chisholm. 1985. Muscle glucose metabolism in exercising rats: comparison with insulin stimulation. *Am. J. Physiol.* 248:E575–E580.

Kahn, B.B., L. Rosetti, H.F. Lodish, and M.J. Charron. 1991. Decreased in vivo glucose uptake but normal expression of GLUT1 and GLUT4 in skeletal muscle of diabetic rats. *J. Clin. Invest.* 87:2197–2206.

Katz, L.D., M.G. Glickman, S. Rapoport, E. Ferrannini, and R.A. DeFronzo. 1983. Splanchnic and peripheral disposal of oral glucose in man. *Diabetes.* 32:675–679.

Livingstone, C., D.E. James, J.E. Rice, D. Hanpeter, and G.W. Gould. 1996. Compartment ablation analysis of the insulin-responsive glucose transporter (GLUT4) in 3T3-L1 adipocytes. *Biochem. J.* 315:487–495.

Lund, S., G.D. Holman, O. Schmitz, and O. Pedersen. 1995. Contraction stimulates translocation of glucose transporter GLUT4 in skeletal muscle through a mechanism distinct from that of insulin. *Proc. Natl. Acad. Sci. USA.* 92: 5817–5821.

Luzio, J.P., B. Brake, G. Banting, K.E. Howell, P. Braghetta, and K.K. Stanley. 1990. Identification, sequencing and expression of an integral membrane protein of the trans-Golgi network. *Biochem. J.* 270:97–102.

Malide, D., N.K. Dwyer, E.J. Blanchette Mackie, and S.W. Cushman. 1997. Immunocytochemical evidence that GLUT4 resides in a specialized translocation post-endosomal VAMP2-positive compartment in rat adipose cells in the absence of insulin. *J. Histochem. Cytochem.* 45:1083–1096.

Marette, A., E. Burdett, A. Douen, M. Vranic, and A. Klip. 1992. Insulin induces the translocation of GLUT4 from a unique intracellular organelle to transverse tubules in rat skeletal muscle. *Diabetes.* 41:1562–1569.

Martin, S., B. Reaves, G. Banting, and G.W. Gould. 1994. Analysis of the co-localization of the insulin-responsive glucose transporter (GLUT4) and the trans-Golgi network marker TGN38 within 3T3-L1 adipocytes. *J. Biochem.* 300:743–749.

Martin, S., J. Tellam, C. Livingstone, J.W. Slot, G.W. Gould, and D.E. James. 1996. The glucose transporter (GLUT4) and vesicle-associated membrane protein-2 (VAMP-2) are segregated from recycling endosomes in insulin-sensitive cells. *J. Cell Biol.* 134:625–635.

Mellman, I., and K. Simons. 1992. The Golgi complex: in vitro veritas? *Cell.* 68: 829–840.

Mukherjee, S., R.N. Ghosh, and F.R. Maxfield. 1997. Endocytosis. *Physiol. Rev.* 77:759–803.

Munoz, P., M. Rosenblatt, X. Testar, M. Palacin, G. Thoidis, P.F. Pilch, and A. Zorzano. 1995. The T-tubule is a cell-surface target for insulin-regulated recycling of membrane proteins in skeletal muscle. *Biochem. J.* 312:393–400.

Nakamura, N., C. Rabouille, R. Watson, T. Nilsson, N. Hui, P. Slusarewicz, T.E. Kreis, and G. Warren. 1995. Characterization of a cis-Golgi matrix protein GM130. *J. Cell Biol.* 131:1715–1726.

Nesher, R., I.E. Karl, and D.M. Kipnis. 1985. Dissociation of effects of insulin and contraction on glucose transport in rat epitrochlearis muscle. *Am. J. Physiol.* 249:C233–C237.

Pascoe, W., K. Inukai, Y. Oka, J. Slot, and D.E. James. 1996. Differential targeting of facilitative glucose transporters in polarized epithelial cells. *Am. J. Physiol.* 271:C547–C554.

Ploug, T., and E. Ralston. 1998. Anatomy of glucose transporters in skeletal muscle: effects of insulin and contractions. *In* Skeletal Muscle Metabolism in Exercise and Diabetes. E.A. Richter, B. Kiens, H. Galbo, and B. Saltin, editors. Plenum Press, New York. 17–26.

Ploug, T., H. Galbo, J. Vinten, M. Jorgensen, and E.A. Richter. 1987. Kinetics of glucose transport in rat muscle: effects of insulin and contractions. *Am. J. Physiol.* 253:E12–E20.

Ploug, T., B.M. Stallknecht, O. Pedersen, B.B. Kahn, T. Ohkuwa, J. Vinten, and H. Galbo. 1990. Effect of endurance training on glucose transport capacity and glucose transporter expression in rat skeletal muscle. *Am. J. Physiol.* 259:E778–E786.

Ploug, T., H. Galbo, T. Ohkuwa, J. Tranum-Jensen, and J. Vinten. 1992. Kinetics of glucose transport in rat skeletal muscle membrane vesicles: effects of insulin and contractions. *Am. J. Physiol.* 262:E700–E711.

Ploug, T., X.X. Han, L.N. Petersen, and H. Galbo. 1997. Effect of in vivo injection of cholera and pertussis toxin on glucose transport in rat skeletal muscle. *Am. J. Physiol.* 272:E7–E17.

Rahkila, P., A. Alakangas, K. Väänänen, and K. Metsikkö. 1996. Transport pathway, maturation, and targeting of the vesicular stomatitis virus glycoprotein in skeletal muscle fibers. *J. Cell Sci.* 109:1585–1596.

Rahkila, P., K. Vaananen, J. Saraste, and K. Metsikko. 1997. Endoplasmic reticulum to Golgi trafficking in multinucleated skeletal muscle fibers. *Exp. Cell. Res.* 234:452–464.

Rahkila, P., V. Luukela, K. Vaananen, and K. Metsikko. 1998. Differential targeting of vesicular stomatitis virus G protein and influenza virus hemagglutinin appears during myogenesis of L6 muscle cells. *J. Cell Biol.* 140:1101–1111.

Ralston, E. 1993. Changes in architecture of the Golgi complex and other subcellular organelles during myogenesis. *J. Cell Biol.* 120:399–409.

Ralston, E., and T. Ploug. 1996a. GLUT4 in cultured skeletal myotubes is segregated from the transferrin receptor and stored in vesicles associated with the TGN. *J. Cell Sci.* 109:2967–2978.

Ralston, E., and T. Ploug. 1996b. Pre-embedding staining of single muscle fibers for light and electron microscopy studies of subcellular organization. *Scanning Microsc. Suppl.* 10:249–260.

Ranvier, L. 1874. Note sur les vaisseaux sanguins et la circulation dans les muscles rouges. *C.R. Soc. Biol.(Paris).* 26:28–31.

Rodnick, K.J., J.W. Slot, D.R. Studelska, D.E. Hanpeter, L.J. Robinson, H.J. Geuze, and D.E. James. 1992. Immunocytochemical and biochemical studies of GLUT4 in rat skeletal muscle. *J. Biol. Chem.* 267:6278–6285.

Roy, D., and A. Marette. 1996. Exercise induces the translocation of GLUT4 to transverse tubules from an intracellular pool in rat skeletal muscle. *Biochem. Biophys. Res. Comm.* 223:147–152.

Sevilla, L., E. Tomas, P. Munoz, A. Guma, Y. Fischer, J. Thomas, B. Ruiz-Montasell, X. Testar, M. Palacin, J. Blasi, and A. Zorzano. 1997. Characterization of two distinct intracellular GLUT4 membrane populations in muscle fiber. Differential protein composition and sensitivity to insulin. *Endocrinology.* 138:3006–3015.

Slot, J.W., H.J. Geuze, S. Gigengack, G.E. Lienhard, and D.E. James. 1991a. Immunolocalization of the insulin regulatable glucose transporter in brown adipose tissue of the rat. *J.Cell Biol.* 113:123–135.

Slot, J.W., H.J. Geuze, S. Gigengack, D.E. James, and G.E. Lienhard. 1991b. Translocation of the glucose transporter GLUT4 in cardiac myocytes of the rat. *Proc. Natl. Acad. Sci. USA.* 88:7815–7819.

Slot, J.W., G. Garruti, S. Martin, V. Oorschot, G. Posthuma, E.W. Kraegen, R. Laybutt, G. Thibault, and D.E. James. 1997. Glucose transporter (GLUT4) is targeted to secretory granules in rat atrial cardiomyocytes. *J. Cell. Biol.* 137:1243–1254.

Smith, R.M., M.J. Charron, N. Shah, H.F. Lodish, and L. Jarett. 1991. Immuno-electron microscopic demonstration of insulin-stimulated translocation of glucose transporters to the plasma membrane of isolated rat adipocytes and masking of the carboxyl-terminal epitope of intracellular GLUT4. *Proc. Natl. Acad. Sci. USA.* 88:6893–6897.

Stefanini, M., C. De Martino, and L. Zamboni. 1967. Fixation of ejaculated spermatozoa for electron microscopy. *Nature.* 216:173–174.

Suzuki, K., and T. Kono. 1980. Evidence that insulin causes translocation of glucose transport activity to the plasma membrane from an intracellular storage site. *Proc. Natl. Acad. Sci. USA.* 77:2542–2545.

Takata, K., O. Ezaki, and H. Hirano. 1992. Immunocytochemical localization of fat/muscle-type glucose transporter (GLUT4) in the rat skeletal muscle: effect of insulin treatment. *Acta Histochem. Cytochem.* 25:689–696.

Tassin, A.M., M. Paintrand, E.G. Berger, and M. Bornens. 1985. The Golgi apparatus remains associated with microtubule organizing centers during myogenesis. *J. Cell Biol.* 101:630–638.

Tokuyasu, K.T. 1980. Immunocytochemistry on ultrathin cryosections. *Histochem. J.* 12:381–403.

Tokuyasu, K.T. 1989. Use of poly(vinylpyrrolidone) and poly(vinylalcohol) for cryoultramicrotomy. *Histochem. J.* 21:163–171.

Wang, W., P.A. Hansen, B.A. Marshall, J.O. Holloszy, and M. Mueckler. 1996. Insulin unmasks a COOH-terminal GLUT4 epitope and increases glucose transport across T-tubules in skeletal muscle. *J. Cell Biol.* 135:415–430.

Wardzala, L.J., and B. Jeanrenaud. 1981. Potential mechanism of insulin action on glucose transport in the isolated rat diaphragm. *J. Biol. Chem.* 256:7090–7093.

White, S., K. Miller, C. Hopkins, and I.S. Trowbridge. 1992. Monoclonal antibodies against defined epitopes of the human transferrin receptor cytoplasmic tail. *Biochim. Biophys. Acta.* 1136:28–34.

Wilson, C.M., and S.W. Cushman. 1994. Insulin stimulation of glucose transport activity in rat skeletal muscle: increase in cell surface GLUT4 as assessed by photolabelling. *Biochem. J.* 299:755–759.

Xu, K.Y., and L.C. Becker. 1998. Ultrastructural localization of glycolytic enzymes on sarcoplasmic reticulum vesicles. *J. Histochem. Cytochem.* 46:419–427.